New insights into the lifestyle of *Allosaurus* (Dinosauria: Theropoda) based on another specimen with multiple pathologies

Christian Foth, Serjoscha Evers, Ben Pabst, Octávio Mateus, Alexander Flisch, Mike Patthey, Oliver W. M. Rauhut

Adult large-bodied theropods are often found with numerous pathologies. A large, almost complete, probably adult Allosaurus specimen from the Howe Stephens Quarry, Morrison Formation (Late Kimmeridgian–Early Tithonian), Wyoming, shows multiple pathologies. Pathologic bones include the left dentary, two cervical vertebrae, one cervical and several dorsal ribs, the left scapula, the left humerus, right ischium, and two left pedal phalanges. These pathologies can be classified as follows: the fifth cervical vertebra, the scapula, several ribs and the ischium are traumatic, and a callus on the shaft of the left pedal phalanx II-2 is traumatic-infectious. Traumatically fractured elements exposed to frequent movement (e.g. the scapula and the ribs) show a tendency to develop pseudarthroses instead of callus healing. The pathologies in the lower jaw and a reduced flexor tubercle of the left pedal phalanx II-2 are most likely traumatic or developmental in origin. The pathologies on the fourth cervical are most likely developmental in origin or idiopathic, that on the left humerus is infectious or idiopathic, whereas left pedal phalanx IV-1 is classified as idiopathic. With exception of the ischium, all traumatic / traumatic-infectious pathologic elements show unambiguous evidences of healing, indicating that the respective pathologies did not cause the death of this individual. Alignment of the scapula and rib pathologies from the left side suggests that all may have been caused by a single traumatic event. The ischial fracture may have been fatal. The occurrence of multiple traumatic pathologies again underlines that large-bodied theropods experienced frequent injuries during life, indicating an active predatory lifestyle, and their survival perhaps supports a gregarious behavior for Allosaurus. Signs of infections are scarce and locally restricted, indicating a successful prevention of the spread of pathogens, as it is the case in extant reptiles (including birds).

New insights into the lifestyle of *Allosaurus* (Dinosauria: Theropoda) based on another specimen with multiple pathologies

Christian Foth[1,2], Serjoscha Evers[2,3], Ben Pabst[4], Octávio Mateus[5,6], Alexander Flisch[7], Mike Patthey[8], Oliver W. M. Rauhut[1,2]

[1] SNBS, Bayerische Staatssammlung für Paläontologie und Geologie, Richard Wagner-Str. 10, D-80333 München

[2] GeoBio-Center, Department of Earth and Environmental Sciences, Ludwig-Maximilians-Universität, Richard-Wagner-Str. 10, D-80333 München, Germany

[3] Department of Earth Sciences, University of Oxford, South Parks Road, Oxford OX1 3AN, UK

[4] Sauriermuseum Aathal, Zürichstr. 69, CH-8607 Aathal-Seegräben, Switzerland

[5] CICEGe, Faculdade de Ciências e Tecnologia, FCT, Universidade Nova de Lisboa, 2829-516 Caparica, Portugal

[6] Museu da Lourinhã, Rua João Luis de Moura, 2530-157 Lourinhã, Portugal

[7] Empa. Swiss Federal Laboratories for Materials Science and Technology, Center for X-ray Analytics, Überlandstrasse 129, CH-8600 Dübendorf, Switzerland

[8] Vetsuisse Fakulty, Universität Zürich, Winterthurerstrasse 260, CH-8057 Zürich, Switzerland

Abstract

Adult large-bodied theropods are often found with numerous pathologies. A large, almost complete, probably adult *Allosaurus* specimen from the Howe Stephens Quarry, Morrison Formation (Late Kimmeridgian–Early Tithonian), Wyoming, shows multiple pathologies. Pathologic bones include the left dentary, two cervical vertebrae, one cervical and several dorsal ribs, the left scapula, the left humerus, right ischium, and two left pedal phalanges. These pathologies can be classified as follows: the fifth cervical vertebra, the scapula, several ribs and the ischium are traumatic, and a callus on the shaft of the left pedal phalanx II-2 is traumatic-infectious. Traumatically fractured elements exposed to frequent movement (e.g. the scapula and the ribs) show a tendency to develop pseudarthroses instead of callus healing. The pathologies in the lower jaw and a reduced flexor tubercle of the left pedal phalanx II-2 are most likely traumatic or developmental in origin. The pathologies on the fourth cervical are most likely developmental in origin or idiopathic, that on the left humerus is infectious or idiopathic, whereas left pedal phalanx IV-1 is classified as idiopathic. With exception of the ischium, all traumatic / traumatic-infectious pathologic elements show unambiguous evidences of healing, indicating that the respective pathologies did not cause the death of this individual. Alignment of the scapula and rib pathologies from the left side suggests that all may have been caused by a single traumatic event. The ischial fracture may have been fatal. The occurrence of multiple traumatic pathologies again underlines that large-bodied theropods experienced frequent injuries during life, indicating an active predatory lifestyle, and their survival perhaps supports a gregarious behavior for *Allosaurus*. Signs of infections are scarce and locally restricted, indicating a successful prevention of the spread of pathogens, as it is the case in extant reptiles (including birds).

Subjects Animal Behavior, Paleontology, Pathology, Veterinary medicine, Zoology

Keywords Archosauria, gregarious behavior, Jurassic, osteomyelitis, paleopathology, pseudarthrosis, Theropoda

Introduction

Palaeopathology is the study of diseases and traumatic injuries in extinct animals and reveals great potential to provide insights into behaviour (e.g. Rothschild & Storrs, 2003), physiology (e.g. Rothschild et al., 2003), life history (e.g. Hanna, 2002) as well as interspecific (e.g. predator-prey relationships) and intraspecific interactions (e.g. intraspecific combats) (e.g. Carpenter, 2000; Tanke & Currie, 2000; Avilla, Fernandes & Ramos, 2004; Farke, 2004; Carpenter et al., 2005; Farke & O'Connor, 2007; Butler et al., 2013). In recent years, the study of osteological pathologies among non-avian dinosaurs has become of great interest, documenting a wide range of different kinds of injuries and diseases, e.g. fractures and stress fractures (Rothschild, 1988; Rothschild, Tanke & Ford, 2001; Hanna, 2002; Anné et al., 2014), amputations (Farke & O'Connor, 2007; Butler et al., 2013), bite marks and scratches (Carpenter, 2000; Tanke & Currie, 2000; Peterson et al., 2009; Bell, 2010), cancer and tumour growth (Rothschild et al., 2003; Arbour & Currie, 2011), developmental disorders (Witzmann et al., 2008) as well as different kinds of microbial infections (Hanna, 2002; Wolff et al., 2009; Witzmann et al., 2011). Of special interest in this respect are non-lethal pathologies, as they can potentially tell us something about the lifestyle of the animal. Especially, large-bodied non-avian theropods are frequently found with numerous fractures, bite marks and infections (Gilmore, 1920; Molnar & Farlow, 1990; Molnar, 2001; Hanna, 2002; Brochu, 2003; Farke & O'Connor, 2007; Rothschild & Molnar, 2008; Bell, 2010; Bell & Coria, 2013),

indicating an active predatory life style predisposed to injuries (Hanna, 2002). The basal tetanuran *Allosaurus* is one of the best-documented dinosaurs in this field of research (e.g. Marsh, 1884; Gilmore, 1920; Moodie, 1923; Petersen, Isakson & Madsen, 1972; Madsen, 1976; Rothschild, 1988; Rothschild & Martin, 1993; Hanna, 2002; Anné et al., 2014). However, only one study, which is based on the almost complete *Allosaurus* specimen MOR 693 ('Big Al') as well as isolated material from the Cleveland-Lloyd Dinosaur Quarry, has studied its pathologies in greater detail and in a comparative approach (Hanna, 2002). Here, we report a second almost complete, probably adult *Allosaurus* specimen from the Upper Jurassic of Wyoming, U.S.A, which possesses several pathologic bones, including the left dentary, two mid-cervical vertebrae, a right cervical rib, several dorsal ribs, the left scapula, the left humerus, the right ischium, and the left pedal phalanges II-2 and IV-1 (Fig. 1). After documentation and diagnosis, the single pathologies of the specimen will be compared with the data from Hanna (2002) and that of other large-bodied theropods, so that the current study provides new insights into the disease patterns and lifestyles of these remarkable predators.

Material and Methods

The *Allosaurus* specimen SMA 0005 ('Big Al 2') was collected from the Upper Jurassic outcrops of the Morrison Formation (Late Kimmeridgian – Early Tithonian) of the Howe Ranch (Howe Stephens Quarry), Big Horn County, Wyoming, by a team of the Sauriermuseum Aathal (Switzerland) in 1996, close to the famous Howe Quarry discovered by Barnum Brown in 1934 (Brown, 1935; Breithaupt, 1997). The almost complete skeleton was found partially articulated and probably represents an adult individual (total body length = 7.6 m), which is about 12% larger than MOR 693 ('Big Al'), which was found only a few hundred meters away.

For classification of different pathologies present in SMA 0005 we follow the nomenclature of Hanna (2002), who classifies osteological abnormalities as 1) traumatic (resulting from traumatic injury), 2) infectious (resulting from viral, bacterial and protozoan infection), 3) traumatic-infectious (resulting from secondary infection of an injured element), 4) developmental (caused by growth disturbance during development), and 5) idiopathic (pertaining to a condition without clear pathogenesis).

Traumatic injuries of bone include fractures and amputations. If these injuries do not cause the immediate death of an animal they are characterized by healing responses, usually in form of callus formation (Cleas, Wolf & Augat, 2000), which is proliferating growth of originally non-mineralized connective tissue to close the gap and stabilize the respective injury (Park et al., 1998; Cleas et al., 2000; Schell et al., 2005). Generally, the callus surrounds the perimeter of the injured bone locally and forms a different superficial structure compared to healthy bone. If the healing process of the injury is not disturbed by secondary infections or interfragmentary movements, the callus is remodelled by zonal lamellar bone after some time (McKibbin, 1978; Park et al., 1998). In case of bone fractures, however, intense mechanical loadings and interfragmentary movements can rupture the bridging callus tissue, including its vessels, resulting in the formation of a pseudarthrosis or 'false joint' (Cleas et al., 2000; Loboa, Beaupré & Carter, 2001; Klein et al., 2003; Strube et al., 2008), which is usually accompanied by chronic pain, and often so by disability (Loboa et al., 2001). However, pseudarthrosis can also result from syntraumatic malunions (Klein et al., 2003).

An osteological abnormality caused by viral, bacterial or protozoan infections is called osteitis. If such infection becomes chronic and affects the bone marrow it is called osteomyelitis (Pschyrembel, 1990), which is usually characterized by comb-like lesions on the bone surface. In extant mammals, tissue-invasive microbial infections are often characterized by locally restricted, subperiostal suppurative abscesses. In later stages, these abscesses can cause necroses of original bone due to an infiltration of pus into the blood vessel system, impairing the blood supply of the local bone area. Such infiltrations can further lead to a spread of microbial pathogens via the blood stream, affecting other skeletal elements (so called haematogenous osteomyelitis) (Ortner & Putschar, 1981; Pschyrembel, 1990; Gross, Rich & Vickers-Rich, 1993). In contrast, extant reptiles (including birds) do not respond to tissue-invasive microbial infections by producing liquid pus (Montali, 1988; Rega, 2012), but instead by exuding fibrin into the infected areas, which forms local fibriscesses (as a type of granuloma), and preventing the spread of the infection via the blood stream (Gomis et al., 1997; Huchzermeyer & Cooper, 2000; Cooper, 2005). Thus, reptiles usually manifest only contiguous osteomyelitis. Besides osteomyelitis, osteitis can also lead to the formation of exostoses, superficial bony outgrowths.

Developmental disorders are pathologies related to ontogenetic abnormalities resulting from inherent genetic defects or growth disturbances, whereas in idiopathic abnormalities the cause of the osteological pathology is unknown (Hanna, 2002).

To study potential internal structures several pathologic bones of SMA 0005 were CT scanned. The left dentary and the left scapula were investigated using a Siemens SOMATOM Sensation Open (CT) system at Vetsuisse Faculty (University of Zurich) with

source: 120 kV, 176 mA, rotation time: 1 s, pitch: 0.55 mm and slice thickness: 0.6 mm. The fifth cervical was scanned with a 450kV X-ray system MG450 (YXLON) and a CITA 101B+ collimated line detector (CITA Systems Inc.) at the Center for X-ray Analytics (EMPA, Swiss Federal Laboratories for Materials Science and Technology) with source: 450 kV, 3.3 mA, focal spot size: 2.5 mm, target: wolfram, 750 projections of 0.04 s over 360°, slice thickness: 0.25 mm. The generated CT data were preceded with help of the 3D reconstruction software package Amira 5.3.3 (Visage Imaging, Inc.). Unfortunately, the foot was firmly installed in the mounted skeleton, so that the pathologic phalanges could not be scanned.

Institutional Abbreviations

BSPG, Bayerische Staatssammlung für Paläontologie und Geologie, München, Germany; **BYU**, Earth Science Museum, Brigham Young University, Provo, U.S.A.; **DINO** Dinosaur National Monument, Vernal, U.S.A.; **MOR**, Museum of the Rockies, Bozeman, U.S.A.; **NCSM**, North Carolina Museum of Natural Sciences, Raleigh, U.S.A.; **SMA**, Sauriermuseum Aathal, Switzerland; **UMNH**, Utah Museum of Natural History, Salt Lake City, U.S.A., (formerly UUVP, University of Utah Vertebrate Paleontology); **USNM**, National Museum of Natural History, (formerly United States National Museum), Smithsonian Institution, Washington, D.C., U.S.A.

Results

Dentary

The anterior end of the left dentary in SMA 0005 is strongly modified. In lateral view, it has the shape of an anterior rosette, similar to the morphology seen in spinosaurid megalosaurs (Stromer, 1915; Charig & Milner, 1997; Sereno et al., 1998). The anterior

part is both dorsally and ventrally expanded, reaching a maximal height at the level of the fifth alveolus. Anteriorly, the alveolar border curves ventrally, forming a convex arch, resulting in a slightly procumbent anterior-most and, to a lesser degree, second alveolus (Fig. 2). Anterior to the first clearly identifiable alveolus, there is another concavity on the medial side of the bone facing anterodorsally, which might represent a further tooth position. If this interpretation were correct, the first tooth of the left dentary in SMA 0005 would be almost anteriorly directed. However, CT data of the dentaries show that the proximal part of the left dentary is formed by compact bone, while respective parts on the right dentary, as well as more distal parts on both dentaries, show repetitive indentations representing deep alveoli. Therefore, it is also possible that the first alveoli of the left dentary were reduced during the healing response to merely externally visible, shallow pits, and that the anterior part of the left dentary was thereafter edentulous. No clear indication of a fracture, bite marks, callus or other lesion are visible, indicating that this pathology happened a long time before the death of the animal, possibly even during its early development. As a consequence of the pathology in the left dentary, the symphysial region of the mandible is dorsoventrally shortened, and when both mandibles are aligned with the ventral border of the symphysis, at least the anterior part of the left alveolar margin would project dorsally well beyond the right alveolar margin.

Cervicals

Within the cervical series of SMA 0005 two cervical vertebrae could be identified as pathologic. The fourth cervical shows a conspicuous, irregularly shaped proliferation of bone originating from the posteromedial side of the left prezygapophysis (Fig. 3A, B). The proliferation is anteroventrally and medially directed and measures c. 9 mm

anteroposteriorly, c 18 mm dorsoventrally and 25 mm lateromedially in its maximum extent. Anteriorly, the proliferation flattens and expands laterally, contacting the ventromedial side of the left prezygapophysis, so that it looks inverted L-shaped from dorsal view. From anterior view it is kidney-shaped with the concave edge facing ventrally. The surface of the structure is overall rugose. A further small anomaly is present medial to the left lateral margin of the spinopostzygapophyseal fossa above the neural canal (Fig. 3C-E). The structure is posteroventrally directed and tapers distally. It measures c. 6 mm anteroposteriorly, c. 9 mm dorsoventrally and c. 11 mm lateromedially. A clear diagnosis of both exostoses is difficult. As no external indicator of a fracture or infection is observable, and as the structures belong to none of the regular parts and processes of the vertebra, the most plausible explanation could be an enthesopathy (= inflammatory ossification of ligamentous or muscular attachments), an osteochondroma (= benign bone tumour) or an idiopathy. Here, the irregular shape of the large anterior exostosis may correspond with the cauliflower-like morphology of an osteochondroma (Murphey et al., 2000).

The neural arch of the fifth cervical shows a severe injury caused by a fracture at the base of the left postzygapophysis (Fig. 4). In external view, the fracture runs around the whole process, indicating the complete rupture of the postzygapophysis. The fracture is surrounded by a large callus on the dorsolateral side, which gives the left postzygapophyseal pedicle a swollen appearance, and follows roughly the course of the epipoprezygapophyseal lamina. While the broken postzygapophyseal fragment seems secondarily well connected to the neural arch medially, the fracture line appears as a gap laterally, separating the callus in an anterior and posterior part, which are not connected to each other. The anterior part of the callus measures c. 38 mm. Anteriorly, it

ends at the level of the posterior edge of the transverse process. The callus shows a stronger lateral (c. 14 mm) than dorsal expansion (c. 8 mm). The posterior part of the callus is smaller and measures c. 19 mm in its anteroposterior dimension. The external surface of both parts of the callus is smooth, without any rugosity. CT data of the specimen show no abnormalities in the bone structure around the injury.

Presacral ribs

Several ribs of SMA 0005 show evidence of traumatic events. In the cervical region, one pathologic rib is found on the right side of the fourth cervical vertebrae (Fig. 5A). In the dorsal region, the fifth rib from the right body side shows a fracture in its distal third. On the left body side, the third, seventh and ninth dorsal ribs show clear evidences of fractures, appearing all in the distal half of the rib, almost on the same level (Fig. 5B). Other ribs from the left side also show deformations on this level. However, as clear fractures cannot be observed, a distinction between a pathologic or taphonomic origin is not possible for the deformed elements. All fractured bones identified show a distinct overlapping connection of both broken elements, sometimes with a slight displacement of the distal end. No callus formation is visible. These observations are consistent with the morphology of pseudarthroses (Cleas et al., 2000; Loboa et al., 2001; Klein et al., 2003).

Scapula

A complete, transverse fracture occurs in the proximal part of the left scapula (Fig. 6). This fracture does not show a regular callus, but some osseous connection of the fractured end to the respective other fragment is apparent. Thus, the proximal fragment, which articulates with the coracoid and the humerus, is laterally displaced, so that it sits

on the distal fragment. The periphery around the distal end of the proximal fragment shows a rough striation in line with the longitudinal axis of the scapula. The lateral displacement may be explained by a number of reasons, including mechanical instability due to the morphology of the scapula as a blade-like element or the nature of the traumatic event that caused the fracture. One possible explanation might be found in the separation of muscle groups on the lateral scapula in a distal part (*M. deltoideus scapularis*) and a more proximal part (*Mm. scapulohumeralis, M. deltoideus clavicularis*), with the boundary between these two regions apparently coinciding with the area of the break in SMA 0005 (see Remes, 2008; Burch, 2014). Thus, the pull of the *M. deltoideus scapularis* would have rotated the distal end of the scapula outwards in respect to the proximal end, possibly accounting for the overlap. Furthermore, the proximal fragment is displaced in that it is rotated ventrally. This tilt is probably caused by the mechanical load of the arm, pulling the fragment it is articulated with down. The malunion of the fracture fragment, once achieved, can hardly be reversed, and the weight of the attached arm together with movements induced by arm use and torso movements related to locomotion of the animal account for a lack of stabilization of the fracture. The maximal overlap between the proximal and distal element is c. 81 mm. CT data of the specimen show that most of the overlapping parts only lie on top of each other, and that only the fracture ends constitute a fused bridge between the fracture elements (Fig. 6D). The overall morphology and the CT data of the fracture are consistent with the morphology of a pseudarthrosis (Cleas et al., 2000; Loboa et al., 2001; Klein et al., 2003). In a preliminary report (Evers et al., 2013), we described a second potential fracture of the scapula in the distal part of the bone. However, a re-examination of the specimen suggests rather a plastic deformation of this structure.

Humerus

The left humerus of SMA 0005 shows an abnormal ulnar condyle (Fig. 7). The ulnar condyle has an irregular surface texture of numerous pits of varying depth, and it has a deep oblique groove toward the anterior aspect of the medial side. Additionally, the ventral surface of the ulnar condyle bears some sharp, trough-like marks. Also, the ulnar condyle of the left element is elongate and thin, contrasting the more rounded morphology usually seen in theropods and also seen in the right element. Therefore, the abnormal form and texture of the left ulnar condyle is interpreted as an idiopathic pathology, although the pits might indicate a potential infection.

Ischium

The right ischium exhibits an oblique fracture located at a midshaft position (Fig. 8). The distal fracture fragment sits on the medial side of the proximal fragment, and is slightly medially rotated. Due to this orientation, there is a distally widening interfragmentary gap between the distal end of the proximal fracture fragment and the proximal part of the distal fracture fragment, which can be best seen in anterior view (Fig, 8B). Consequentially, the end of the proximal fragment forms a laterally projecting tip. The gap is partially filled with matrix, which shows that is was internally not closed by connective tissue when the animal died. The fracture line can be traced almost around the entire shaft of the ischium (Fig. 8B-E). However, toward the proximal end of the fracture, the fragments are well connected on the anteromedial side. Because no clear callus structure is visible, and because the fracture line is at no point bridged by cortical bone, it is possible, that either the trauma caused only incomplete fracturing and no healing took place (which would indicate trauma-related death of the animal), or that breakage of the bone occurred post-mortem. Another possibility is that the fracture was

complete, and that the anteromedially located connection of the fragments was secondarily achieved. In this case, the structure would fulfill the criteria of a developing pseudarthrosis (see Cleas et al., 2000; Loboa et al., 2001; Klein et al., 2003). On the anterior side of the fractured area, the cortical surface is disturbed by a large trace of small, interconnected depressions with irregular size, shape, and depth. The traces continue well beyond the fracture almost to the ischial boot. As similar traces appear also on the surface of other bones we interpret this structure as most probably taphonomic in origin (see discussion, Fig. 5C, D).

The left ischium shows a slight swelling and possible associated fracture line at the same level as the right element (Fig. 8A). However, parts of the possible pathology are obscured by a reconstruction of the lateral bone surface in this part. Thus, if our observation is correct, it would be impossible to say if the bone was completely or only partially fractured, and if any healing occurred. However, due to the present uncertainty regarding this structure, we avoid further interpretations.

Foot

The pedal phalanx II-2 of the left foot has a bulbous callus covering about two-thirds of the element (Fig. 9A-D). The callus is located at the proximal part of the phalangeal shaft, and does not reach both the proximal and distal articulation facets. In the mid-shaft area, the callus surrounds the phalanx body almost entirely. Toward the proximal articulation, the callus forms a groove-like channel with a sharp and step-like edge, which circumferences the medial, dorsal, and lateral parts of the callus. Towards the distal articulation, the callus is laterally complanate and hence approaching the regular morphology again, while the medial aspect is strongly swollen. The ventral side of the

proximal end is also strongly inflated, exhibiting a c. 5 mm thick bulge. The surface of the callus is generally irregular, while the degree of irregularity is reducing towards the distal part of the element, and weaker developed than in comparative specimens (Hanna, 2002; see discussion).

Compared to the non-pathological pedal phalanx II-2 of the right foot (Fig, 9E), the extensor tubercle is almost completely reduced in the left pedal phalanx II-2 with the most proximal point ending approximately 40 mm anteriorly in relation to the ventral flexor heel (see Fig, 9A, C, D). However, the surface structure in the respective area of the phalanx is not indicative of taphonomic deformation or erosion. Therefore, this anomaly likely represents a pathologic structure. It is perhaps developmental in origin or results from a healed trauma that happened a long time before the death of the animal.

Several depressions could be observed in this bone, penetrating the callus (Fig. 9B, C). The largest depressions appear posteromedially and are several millimetres deep. Here, the outer margin of the more posterior depression measures c. 6 mm by 10 mm and faces posteromedially. The second depression lies anteroventrally in respect to the former, and faces medially. Its outline is circular and measures c. 7 mm by 7 mm. Both depressions possess a distinct rim. The ventral aspect of the callus also shows several small round to oval-shaped depressions. If these depressions underlie a pathologic origin, the current morphology is consistent with lesions caused by osteomyelitis (Ortner & Putschar, 1981; Pschyrembel, 1990; Rothschild & Martin, 2006).

In the left pedal phalanx IV-1, there are two bulbous swellings on the lateral side (Fig. 9F). One is positioned underneath and posteroventral to the lateral ligament pit, another one is situated at the posterolateral side near the proximal articulation. The anterior swelling follows the slightly sinuous curvature of the ventral side of the bone in lateral view, which is the result of the constricted phalangeal shaft between the proximal and distal joints, which are both dorsoventrally expanded in relation to the shaft. The posterior swelling parallels the posterolateral and lateral margin of the proximal articulation, and is therefore vertically oriented. The swellings are separated by a small oblique gap, under which the bone seems to have retained its usual form. Both swellings have a smooth surface structure not different from other parts of the bone, but are not found on the same element of the right foot and are therefore abnormal. The swellings are different from the callus on the left pedal phalanx II-2, as they have a clearly delimited and abrupt border to either side. As additionally no lesions are found and a fracture line is absent, the pathology on the left pedal phalanx IV-1 is classified as idiopathic.

Discussion

Identification and cause of pathologies

According to the scheme of Hanna (2002), the pathologic elements of SMA 0005 can be classified as follows: the fifth cervical vertebra, the scapula, several ribs and right ischium are traumatic, and the callus structure of the left pedal phalanx II-2 is traumatic-infectious. In contrast, the supposed pathologies in the lower jaw and in the reduced flexor tubercle of the left pedal phalanx II-2 cannot be assigned to a certain type of this scheme, as they show evidence of advanced healing. They are most likely traumatic or

374 developmental in origin. The same is true for the abnormal outgrowths in the neural
375 arch of the fourth cervical, which are most likely developmental in origin or idiopathic.
376 The pathology on the left humerus is infectious or idiopathic, whereas the left pedal
377 phalanx IV-1 is classified as idiopathic. With exception of the ischium, all traumatic /
378 traumatic-infectious pathologic elements show unambiguous evidences of healing,
379 indicating that the respective pathologies did not cause the death of SMA 0005. The role
380 of the ischial fracture as a possible cause of death will be discussed below.
381
382 The deformed anterior end of the left dentary of SMA 0005 is most likely pathologic, but
383 no obvious lesions are developed. This indicates that the supposed pathology was
384 probably completely healed and happened long before the animal died. A pathology in
385 the anterior part of the dentary is also found in the *Allosaurus* specimen USNM 2315
386 (Gilmore, 1920; Tanke & Currie, 2000; Molnar, 2001). As in SMA 0005, the symphysial
387 region is strongly deformed, leading to a concavity in the anterior part of the dentary,
388 which is bordered anteriorly by a dorsally pointing, hook-like projection. The anterior
389 alveoli are completely resorbed so that the symphysial region is edentulous. According
390 to Gilmore (1920) and Tanke & Currie (2000) the anterior end of the dentary in USNM
391 2315 was probably bitten off and then heavily remodelled during the healing process. As
392 no sign of other pathologic deformations are visible in the anterior end of the dentary,
393 the supposed trauma happened probably long before the death of the animal, too.
394 Assuming a similar scenario for the supposed pathology in SMA 0005, both specimens
395 may indicate face-biting behaviour in *Allosaurus*, which was previously also
396 hypothesized for other large-bodied theropods (e.g. *Sinraptor*, *Albertosaurus*,
397 *Daspletosaurus*, *Gorgosaurus* and *Tyrannosaurus*), including in juveniles of some of these
398 taxa (Tanke & Currie, 2000; Peterson et al., 2009; Bell, 2010). Another example of a

399 remodeled alveolus with possible traumatic origin was recently described for a single
400 maxilla of the basal tetanuran *Sinosaurus* (= "*Dilophosaurus sinensis*") (Xing et al., 2013).
401 However, it is also possible that the abnormal shape of the dentary in SMA 0005 results
402 from developmental malformation or a fracture that happened in earlier ontogeny,
403 which left no remaining traces.
404
405 The deformation of the anterior end of the dentary has implications for the structure
406 and function of the mandibular symphysis in *Allosaurus*. As pointed out by Holliday &
407 Nesbitt (2013), most basal theropod dinosaurs have a very simple mandibular
408 symphysis that consists of a simple flattened medial area of the anterior end of the
409 dentary. However, even in such an osteologically simple structure the actual union of the
410 left and right mandible by connective tissue can be quite variable (see Holliday et al.,
411 2010). The deformation of the left, but not the right mandible in SMA 0005 indicates that
412 there was no very tight junction between the two mandibular rami, and the symphysis
413 and the jaws as a whole functioned despite the different morphologies and resulting
414 differences in the level of the alveolar margins in the left and right mandible. This is also
415 supported by the deformation seen in USNM 2315, which also affected the mandibular
416 symphysis.
417
418 Another interesting aspect of the pathologic dentary of SMA 0005 is its similarity with
419 dentaries of spinosaurid megalosaurs. As there are no direct indications of pathology in
420 the bone itself, and the pathologic nature can only be inferred by comparison with the
421 other dentary, which shows a more typical morphology for *Allosaurus*. This element, if
422 found isolated, would probably not have been classified as *Allosaurus*. This has
423 happened with the dentary USNM 2315, which was originally described as a new

424 species, *Labrosaurus ferox*, by Marsh (1884). Thus, caution is needed when evaluating
425 the systematic position of isolated elements to rule out possible pathologies.
426
427 The most common pathology in the axial skeleton of dinosaurs is the fusion of single
428 vertebrae, which often appears in the caudal series. Possible causes of vertebral fusion
429 are e.g. congenital abnormality (e.g. Witzmann et al., 2008), infections (Rothschild, 1997;
430 Rothschild & Martin, 2006), malformations during the healing process of a trauma
431 (Rothschild, 1997; Butler et al., 2013), diffuse idiopathic skeletal hyperostosis (DISH)
432 (Rothschild, 1987; Rothschild & Berman, 1991) or spondyloarthropathy (Rothschild &
433 Martin, 2006; Witzmann et al., 2014). No evidence of vertebral fusion is found in SMA
434 0005.
435
436 Like in the *Allosaurus* specimen MOR 693, the dorsal neural spines of SMA 0005 show
437 irregular-shaped exostoses, which were diagnosed by Hanna (2002) as idiopathic
438 pathological ossification of interspinous ligaments. However, little research has been
439 done on the classification of ossified ligaments and other soft tissues in dinosaurs. In
440 ornithopods and dromeosaurid theropod dinosaurs, ossified tendons are found to stiffen
441 parts of the axial skeleton, and these structures are commonly not interpreted as
442 pathologic (e.g. Ostrom, 1969; Norell & Makovicky, 1999; Organ, 2006). However, in
443 many theropod dinosaurs, rugose outgrowths are found on the anterior and posterior
444 sides of the neural spine, which are thought to be part of ossified prespinal and
445 postspinal ligaments, respectively. These structures occur more frequently on larger
446 specimens (e.g. *Allosaurus* BYU 725/12901, BYU 725/12902, BYU 725/13051, UMNH VP
447 8365, UMNH VP 13813; *Acrocanthosaurus* SMU 74646, Harris 1998; cf. *Spinosaurus*
448 BSPG 2006 I 57), although there are also smaller specimens with such ossification (e.g.

449 *Allosaurus* UMNH VP 7341, DINO 11541). In individuals preserving an articulated or
450 associated vertebral series, no clear pattern of intervertebral tendon ossifications can be
451 observed. In *Neovenator*, the posterior cervical vertebrae show ossifications at the
452 apexes of the neural spines, and most dorsal vertebrae show such structures (Brusatte,
453 Benson & Hutt, 2008), while in *Baryonyx*, a mid-cervical vertebra (BMNH R9951) shows
454 relatively large ossifications, whereas more posterior positioned vertebrae lack such
455 structures and only show rugose attachment sites for the respective ligaments on the
456 neural arch (Charig & Milner, 1997). In some cases, the interspinal ossifications have
457 been suggested to be of diagnostic and thus taxonomic value (Chure, 2000). The above
458 cases show that ligament ossifications in dinosaurs are frequently not interpreted as
459 pathologic, and because many theropods show ossifications of at least the attachment
460 areas of interspinal ligaments, we advocate that they should be regarded as non-
461 pathologic, pending more detailed research on the topic.
462
463 However, the exostoses found in the fourth cervical of SMA 0005 differ in their position
464 and morphology from the examples mentioned above. Here, the strongly irregular shape
465 of the anterior exostosis resembles the morphology of an osteochondroma, which
466 represents the most common type of bone tumours in humans (Murphey et al., 2000;
467 Sekharappa et al., 2014). In captive wild extant mammals and reptiles (including birds),
468 however, the development of tumours is rather rare (Ratcliffe, 1933; Effron, Griner &
469 Benirschke, 1977; Huchzermeyer, 2003). Thus, it is not surprising that the unambiguous
470 diagnosis of tumours in dinosaurs is limited to only a few cases (e.g. Rothschild et al.,
471 1998; Rothschild, Witzke & Hershkovitz, 1999; Rothschild et al., 2003; Arbour & Currie,
472 2011; Rega, 2012). Due to the restricted knowledge of tumour formation in dinosaurs in
473 general, this diagnosis has to be seen with caution. However, if the diagnosis is correct,

the anterior exostosis found in the fourth cervical of SMA 0005 represents the third case of an osteochondroma in dinosaurs (Rega, 2012). The smaller, more regular-shaped exostosis on the posterior side of the neural arch does not fulfil the criteria for a bone tumour. One possible explanation for these structures could be an inflammatory ossification of the *ligamentum elasticum interlaminare*, which attaches right above the neural canal of cervical vertebrae (Tsuihiji, 2004), probably affecting the neck mobility. However, if none of the presented diagnosis is correct, both exostoses have to be classified as idiopathic.

Evidence for traumatic pathologies in the vertebral column is also rare in dinosaurs. Carpenter et al. (2005) describes an anterior caudal of *Allosaurus* with a possible puncture in the left transversal process, which was most likely injured by a *Stegosaurus* tail spike, indicating a predator-prey relationship between both dinosaurs. Traumatic caudals found in the basal sauropodomorph *Massospondylus* (Butler et al., 2013) and the hadrosaur *Edmontosaurus* (Carpenter, 2000) probably result from unsuccessful attacks of large-bodied theropods, indicating active hunting behaviour in the latter, while an injured caudal in the abelisaurid *Majungasaurus* (Farke & O'Connor, 2007) may indicate cannibalistic behaviour. In contrast, the traumatic fracture found in the fifth cervical of SMA 0005 probably results from a serious accident. Although the whole left postzygapophysis was basically broken, the trauma shows evidence of healing in form of a callus, indicating the survival of the accident. A possible explanation for such a rather unusual break might be found in the importance of the neck in hunting behaviour in large theropods (e.g. Snively & Russell, 2007a,b; Snively et al., 2013). Thus, the injury might have resulted from a failed hunting attack or from struggling prey, in which case this represents further evidence for active hunting in *Allosaurus* (see also Carpenter et

al., 2005). However this may be, the severity of the injury most probably had a serious affect on the neck mobility of the specimen (see Snively et al., 2013).

Fractured or infected presacral ribs are one of the most common pathologies found within theropods (Molnar, 2001), in which, however, cervical ribs are less affected than dorsal elements. Pathologic cervical ribs are reported for *Megalosaurus* (Tanke & Rothschild, 2002), *Allosaurus* (Petersen et al., 1972) and *Tyrannosaurus* (Brochu, 2003), whereas corresponding dorsal rib pathologies are found in various large-bodied theropods like the abelisaurid *Majungasaurus* (Farke & O'Connor, 2007), the allosauroids *Acrocanthosaurus* (Harris, 1998), *Allosaurus* (Molnar, 2001; Hanna, 2002; Rothschild & Tanke, 2005), *Mapusaurus* (Bell & Coria, 2013) and *Sinraptor* (Currie & Zhao, 1993) and the tyrannosaurids *Albertosaurus* (Bell, 2010), *Gorgosaurus* (Lambe, 1917) and *Tyrannosaurus* (Brochu, 2003; Rothschild & Molnar, 2008). The examples mentioned above show different kinds of pathologies, i.e. trauma-related callus formations (Harris, 1998; Hanna, 2002; Brochu, 2003), pseudarthroses (Harris, 1998; Brochu, 2003; Rothschild & Molnar, 2008; Bell, 2010) or lesions by microbial infections (Harris, 1998; Hanna, 2002; Brochu, 2003; Bell & Coria, 2013), in which the latter could be the result of secondary infections of the injury. Hanna (2002) further describes the formation of idiopathic spiculae on two fractured dorsal ribs in the *Allosaurus* specimen MOR 693. In SMA 0005, all pathologic ribs show evidence for traumatic-related pseudarthroses. Here, the pseudarthrosis as a healing response (rather than callus healing) in the cervical rib results most likely from regular neck movements (Snively & Russell, 2007a; Snively et al., 2013), whereas the pseudarthroses found in the dorsal ribs were probably caused by constant movement of the ribcage during breathing (Claessens, 2009a,b) or due to thorax movements during locomotion (see Mallison, 2010).

The fractured scapula shows a clear case of a pseudarthrosis as healing response, which resulted from the apparent malunion of the fractured elements. Mechanical loading is additionally likely, as the proximal fragment, which is articulated with the rest of the arm, is tilted ventrally. The extent of the malunion may be indicative of syn-traumatic displacement, which potentially indicates great destructive force acting upon the element. Accordingly, the left arm in SMA 0005 was likely dysfunctional after the trauma. Other examples of pathologic scapulae in theropods can be found in the *Allosaurus* specimen USNM 4734 (Gilmore, 1920; Rothschild, 1997; Molnar, 2001) and in *Yangchuanosaurus* (Xing et al., 2009). The scapula of USNM 4734 shows a strong, arched dislocation between both fragments, in which the proximal element developed a spine-like exostosis on the ventral margin of the projecting portion of the proximal fragment (Gilmore, 1920; Rothschild, 1997). In contrast, the injury of the scapula in *Yangchuanosaurus* shows callus formation as healing response (Xing et al., 2009), indicating an incipient fracture. Other examples of pathologic scapulae seem not to be related to traumatic events, but with the development of exostoses [e.g. *Acrocanthosaurus* (NCSM 14345, pers. obs.) and *Neovantor* (Brusatte et al., 2008)], idiopathic lesions [e.g. *Allosaurus* (MOR 693; Hanna, 2002)] and infectious lesions in relation to osteomyelitis [e.g. *Allosaurus* (UUVP 1528, UUVP 5599, Molnar, 2001; Hanna, 2002)].

Because the injuries of the left scapula and the dorsal ribs from the left side are present at almost the same level of the thorax, it is possible that these traumas happened in one single event, e.g. a serious fall, or a defensive blow from a sauropod tail. This scenario would be even more probable if the deformations found in the other dorsal ribs from the

549 left side have a traumatic origin. However, as stated above, this cannot currently be
550 confirmed, as they cannot be distinguished from taphonomic deformations. Multiple rib
551 fractures from one thorax side are also documented in *Acrocanthosaurus* (Harris, 1998),
552 *Allosaurus* (Hanna, 2002) and *Tyrannosaurus* (Brochu, 2003), possibly resulting from
553 one single traumatic event.
554
555 The most complex pathology appears in the left pedal phalanx II-2, including a reduced
556 flexor tubercle, a callus formation of the phalangeal shaft, and several lesions
557 penetrating the callus. The origin of the reduced flexor tubercle remains speculative,
558 possibly being developmental in origin or resulting from a healed trauma. However, as
559 the flexor tubercle in its normal condition should prevent the hyperextension of pedal
560 phalanges, it is possible that the reduced process in SMA 0005 was not able to fulfil this
561 task properly, leading to a frequent overloading of pedal muscles and ligaments. Thus, it
562 is possible that this pathology is physically linked to the callus formation in the proximal
563 portion of the phalangeal shaft. This type of pathology is very common in theropods
564 (Madsen, 1976; Rothschild, 1988; Rothschild et al., 2001; Rothschild & Tanke, 2005;
565 Farke & O'Connor, 2007; Bell, 2010; Zanno et al., 2011; Anné et al., 2014), and probably
566 a result of stress fractures related to strenuous activities (Rothschild et al., 2001;
567 Rothschild & Tanke, 2005). The additional penetration of the callus by several lesions
568 indicate a secondary infection of the pedal phalanx, perhaps caused by a syn-traumatic
569 injury of adjacent soft tissue, through which microbial pathogens got access to the bone
570 and cause contiguous osteomyelitis. Thus, the callus pathology is most likely traumatic-
571 infectious. Secondary infections of callus structures in, as well as infections not clearly
572 linkable to fractures, seem to be common in pedal phalanges of *Allosaurus* (MOR 693,
573 UUVP 1657, UMNH VP 6295, UMNH VP 6284, UMNH VP 10755, UMNH VP 6287, UMNH

574 VP 6299). In two specimens (MOR 693; UUVP 1657), the secondary infections led to
575 colossal exostoses, causing chronic pain and restriction in the locomotion.
576
577 The cause for the abnormalities of the left humerus and left pedal phalanx IV-1 are
578 unknown, although the pits found on the ulnar condyle of the left humerus might result
579 from an infection.
580
581 The most severe and potentially fatal pathology occurs in the ischium, which most likely
582 represents a traumatic fracture. Pathologies in the pelvic region are not often
583 documented in theropods and usually restricted to the ilium (Molnar, 2001; Hanna,
584 2002; Bell & Coria, 2013). In the *Allosaurus* specimen UUVP 5985, the ilium is fused with
585 the ischium (Hanna, 2002). However, an ischial fracture is to our knowledge not
586 documented within theropods so far. The fracture of the right ischium exhibits a large
587 interfragmentary gap with a projecting fragment on the lateral side. Because
588 unambiguous healing responses are absent around the fracture, the possibility that the
589 ischium was broken post-mortem has to be considered. However, scenarios in which a
590 skeletal element with a designated long axis fractures in the oblique way described
591 above are hard to come by, and we think the most parsimonious explanation for the
592 observed fracture is a traumatic event during life. This is perhaps supported by the
593 presence of sandy sediment matrix in the interfragmentary gap, as a void would be
594 expected to be filled by different material if the fracture was the result of stress related
595 to tectonic activity. Although no callus structure is found around the fracture, its absence
596 per se cannot be seen as a clear indicator for the lack of a healing response, as the
597 integration of the ischium in a complex network of locomotor musculature (Carrano &
598 Hutchinson, 2002; Hutchinson et al., 2005) would predict intense motion along the

fracture, favoring the formation of a pseudarthrosis (Cleas et al., 2000; Loboa et al., 2001). As seen in the scapula, large parts of the fracture line can remain unfused in a pseudarthrosis, and the fragments can be adhered at the end points of overlapping fracture fragments. In SMA 0005, the periphery of the connective bone in the scapula is structurally marked by fine striations and modifications from the smooth surface of healthy bone. Unfortunately, the irregular texture of the ischium, which we interpret as taphonomic (see below), prevents an assessment of the bone structure around the area where the ischium fragments meet, as the pattern would have overprinted the original bone surface structure. Therefore, it cannot be clarified if the connection of the fragments is the result of incomplete fracturing, or a secondary bridging due to a healing response. As experimental studies on animal fractures have shown that overhanging fracture ends tend to be resorbed during the healing process (Loboa et al., 2001), the presence of a laterally projecting fragment indicates that the healing process, if already started, was still in an early phase, supporting the hypothesis that the trauma happened shortly before the animal died, and is accordingly a possible cause of death. It is likely that the locomotion ability of SMA 0005 was significantly limited or even inhibited by the injury, consequentially affecting life traits like its hunting success. The reason for the traumatic event remains speculative, although it must have been a forceful incident.

The irregular cortical texture found around the ischial fracture is probably not pathologic. The right pubis shows also large traces of similar structure. Smaller traces can be found in the right coracoid, both scapulae, the left humerus, the left ischium, the left pubis and the left fibula (Fig. 5C, D). The structures differ in their morphology from the supposed lesions found the in right pedal phalanx II-2, as they possess a very irregular outline with a weak margin and a complex inner topography, which is

composed of interconnected round pits with irregular size and depth (c. 1 to 3 mm). This morphology is similar to the superficial pits found on various sauropod bones from the Morrison Formation, which are most likely taphonomic in origin (Fiorillo, 1998; Hasiotis, Fiorillo & Hanna, 1999). Possible causes for these traces are bone corrosion due to soil acidity (Fiorillo, 1998) or scavenging by insect larvae (Hasiotis et al., 1999).

Implications for paleobiology and lifestyle

The number of pathologic specimens in general and the number of pathologies within fairly complete *Allosaurus* individuals suggest that members of this taxon had an active lifestyle predisposed to injury. Most pathologies found seem to be traumatic in origin, but only few show evidence of secondary infection (Molnar, 2001). This either suggests that inflamed wounds quickly caused death, leaving no osteological traces, or that the immune defence of these animals was successful in prohibiting infections. Oftentimes injuries were indeed survived, as evidence for healing responses are abundant in the theropod fossil record. In previous studies (e.g. Hanna, 2002; Butler et al., 2013; Vittore & Henderson, 2013) mammalian immune response has often been used as a model for explaining pathologic structures thought to be related to tissue-invasive microbial infections in non-avian dinosaur taxa. However, while the mammalian immune response to such infections usually is the formation of suppurative abscesses, extant reptiles (including birds) form small cysts of fibrin (fibriscesses) at the sources of infection, which tend to calcify in advance stages (Montali, 1988; Gomis et al., 1997; Huchzermeyer & Cooper, 2000; Cooper, 2005; Rega, 2012). Applying the extant phylogenetic bracket, a reptile-like immune response should be suspected for tissue-invasive microbial infections in non-avian dinosaurs, too. Consequently, application of a mammalian model for infectious pathologies in non-avian dinosaurs should be avoided

649 (see Arbour & Currie, 2011; Rega, 2012). As the localization of pathogens in fibriscesses
650 successfully prevents haematogenous osteomyelitis in reptiles, the risk of lethal
651 infections due to the spread to other body regions is minimized (Rega, 2012). This is
652 supported by the fact that theropods show only very localized indications for infections
653 (Molnar, 2001).
654
655 The severity of pathologies in SMA 0005 and other *Allosaurus* specimens (Gilmore,
656 1920; Molnar, 2001; Hanna, 2002) points to a frequent exposure to hazardous situations.
657 This might be seen as evidence for an active predatory life style. If this is accepted, many
658 of the traumatic pathologies found could be the result of hunting accidents (see e.g.
659 Carpenter et al., 2005). Some of the pathologies seen in *Allosaurus*, like the broken
660 cervical postzygapophysis and scapula of SMA 0005, the hypertrophied pedal phalanx of
661 MOR 693 (Hanna, 2002) and UMNH 1657 (Madsen, 1976; Hanna, 2002), or the fibula of
662 USNM 4734 (Gilmore, 1920) can be expected to severely limit the movement,
663 manoeuvrability, and speed of the animals. This in turn should affect the hunting success,
664 but also intra- and interspecific competition for various other resources (water,
665 territories, captured prey and carrion) of such an individual, which would be expected
666 to mean certain death within a relatively short period of time. This is especially true for
667 animals with solitary behavior. Indeed, the broken ischium qualifies as a strongly
668 limiting and severe injury, and is potentially related to the death of SMA 0005. However,
669 the number of cases of advanced healing for severe injuries within various *Allosaurus*
670 specimens (including SMA 0005) might be an indication of social behaviour, in which
671 prey was shared among individuals of a group. Although stratigraphic and taphonomic
672 information is not provided in detail for all *Allosaurus* remains, this taxon represents the
673 most abundant theropod within the Morrison Formation, and oftentimes appears with

several specimens within near proximity to one another (see Gilmore, 1920; Madsen, 1976; Foster, 2003; Loewen, 2009), supporting a possible gregarious behavior. Within theropod dinosaurs, similar behavior has been further hypothesized for the coelophysoids *Coelophysis* (Colbert, 1989) and *Syntarsus* (Raath, 1990), the carcharodontosaurid *Mapusaurus* (Coria & Currie, 2006), the ornithomimosaur *Sinornithomimus* (Kobayashi & Lü, 2003; Varricchio et al., 2008), and the tyrannosaurids *Albertosaurus* (Currie, 2000; Currie & Eberth, 2010) and *Daspletosaurus* (Currie et al., 2005), which were all found in (nearly) monospecific assemblages. Although monospecific assemblages are scarce in the Morrison Formation (Foster, 2003; Gates, 2005), at least the Cleveland-Lloyd Dinosaur Quarry is by far dominated by *Allosaurus*. In spite of repeated taphonomic and sedimentological investigations of the quarry (Bilbey, 1998, 1999; Gates, 2005), the abundance of *Allosaurus* has not been satisfactorily explained, so that a gregarious scenario should not be ruled out at this point.

Conclusions

The *Allosaurus* SMA 0005 represents a further specimen of this taxon with multiple pathologies, which were mostly traumatic in origin and pertain to all body regions (i.e. skull, axial skeleton, pectoral and pelvic girdle, and extremities). Traces of healing responses in all pathologic bones but the ischium suggest the survival of accidents and infections, but also an active predatory lifestyle predisposed to injury. The scarcity and local restriction of infectious pathologies is in agreement with a reptile-like immune response preventing the spread of infections via the blood stream. The survival of injuries affecting the physical fitness in *Allosaurus* may indicate gregarious behavior. However, verification of this hypothesis would require more direct evidence, like an

699 unambiguous find of a group or direct trackway evidence (e.g. McCrea et al., 2014). The
700 probable fracture in the ischium was potentially fatal, as no advanced traces of healing
701 could be identified.
702
703 **Acknowledgements**
704 We would like to thank Hans 'Kirby' Siber, Thomas Bolliger (both Sauriermuseum
705 Aathal) and entire Aathal team for access to SMA 0005 and logistic support. We further
706 thank Philipp Schütz (EMPA) for assisting during the CT scans, Randy Irmis and Carrie
707 Levitt-Bussian (both Utah Museum of Natural History), Brooks Britt and Rodney Scheetz
708 (both Brigham Young University), and Jack Horner and John Scanella (Museum of the
709 Rockys) for access other *Allosaurus* material as well as Vince Schneider and Lindsay
710 Zanno (both North Carolina Museum of Natural Sciences) for sharing pictures of
711 *Acrocanthosaurus*, and Roger Benson (University of Oxford) for sharing pictures of
712 *Neovenator*. Finally, we want to acknowledge Mark Loewen (Utah Museum of Natural
713 History), Richard Butler (University of Birmingham) and Judith Engmann (Medizinische
714 Hochschule Hannover) and for discussions. This study was supported by the
715 Volkswagen Foundation under grant I/84 640 (to O.W.M.R.).
716
717 **References**

718 Anné J, Edwards NP, Wogelius RA, Tumarkin-Deratzian AR, Sellers WI, van Veelen A,
719 Bergmann U, Sokaras D, Alonso-Mori R, Ignatyev K et al. 2014. Synchrotron imaging
720 reveals bone healing and remodelling strategies in extinct and extant vertebrates.
721 *Journal of the Royal Society Interface* 11:1-10.

722 Arbour VM, Currie PJ. 2011. Tail and pelvis pathologies of ankylosaurian dinosaurs.
723 *Historical Biology* 23:375-390.

724 Avilla LS, Fernandes R, Ramos DFB. 2004. Bite marks on a crocodylomorph from the
725 Upper Cretaceous of Brazil: evidence of social behavior? *Journal of Vertebrate*
726 *Paleontology* 24:971-973.

727 Bell PR. 2010. Palaeopathological changes in a population of *Albertosaurus sarcophagus*
728 from the Upper Cretaceous Horseshoe Canyon Formation of Alberta, Canada.
729 *Canadian Journal of Earth Sciences* 47:1263-1268.

730 Bell PR, Coria RA. 2013. Palaeopathological survey of a population of *Mapusaurus*
731 (Theropoda: Carcharodontosauridae) from the Late Cretaceous Huincul Formation,
732 Argentina. *PLoS ONE* 8:e63409.

733 Bilbey SA. 1998. Cleveland-Lloyd Dinosaur Quarry - age, stratigraphy and depositional
734 enviroments. *Modern Geology* 22:87-120.

735 Bilbey SA. 1999. Taphonomy of the Cleveland-Lloyd Dinosaur Quarry in the Morrison
736 Formation, central Utah - a lethal spring-fed pond. In: Gillette DD ed. *Vertebrate*
737 *Paleontology in Utah*. Salt Lake City: Miscellaneous Publication, 121-133.

738 Breithaupt BH. 1997. Howe Quarry. In: Currie PJ, Padian K eds. *Encyclopedia of*
739 *Dinosaurs*. San Diego: Academic Press, 355-356.

740 Brochu CA. 2003. Osteology of *Tyrannosaurus rex*: insights from a nearly complete
741 ckeleton and high-resolution computed tomographie analysis of the skull. *Society of*
742 *Vertebrate Paleontology Memoir* 7:1-138.

743 Brown B. 1935. Sinclair dinosaur expedition, 1934. *Natural History* 36:2-15.

744 Brusatte SL, Benson RBJ, Hutt S. 2008. The osteology of *Neovenator salerii* (Dinosauria:
745 Theropoda) from the Wealden Group (Barremian) of the Isle of Wight. *Monograph*
746 *of the Palaeontological Society* 162:1-75.

747 Burch SH. 2014. Complete forelimb myology of the basal theropod dinosaur *Tawa hallae*
748 based on a novel robust muscle reconstruction method. *Journal of Anatomy*
749 225:271-297.

750 Butler RJ, Yates AM, Rauhut OWM, Foth C. 2013. A pathological tail in a basal
751 sauropodomorph dinosaur from South Africa: evidence of traumatic amputation?
752 *Journal of Vertebrate Paleontology* 33:224-228.

753 Carpenter K. 2000. Evidence of predatory behavior by carnivorous dinosaurs. *Gaia*
754 15:135-144.

755 Carpenter K, Sanders F, McWhinney LA, Wood L. 2005. Evidence for predator-prey
756 relationships. Examples for *Allosaurus* and *Stegosaurus*. In: Carpenter K ed. *The*
757 *carnivorous dinosaurs*. Bloomington: Indiana University Press, 325-350.

758 Carrano MT, Hutchinson JR. 2002. Pelvic and hindlimb musculature of *Tyrannosaurus*
759 *rex* (Dinosauria: Theropoda). *Journal of Morphology* 253:207-228.

760 Charig AJ, Milner AC. 1997. *Baryonyx walkeri*, a fish-eating dinosaur from the Wealden of
761 Surrey. *Bulletin of the Natural History Museum Geology* 53:11-70.

762 Chure DJ. 2000. A new species of *Allosaurus* from the Morrison Formation of Dinosaur
763 National Monument (UT-CO) and a revision of the theropod family Allosauridae.
764 Columbia University.

765 Claessens LPAM. 2009a. A cineradiographic study of lung ventilation in *Alligator*
766 *mississippiensis*. *Journal of Experimental Zoology* 311A:563-585.

767 Claessens LPAM. 2009b. The skeletal kinematics of lung ventilation in three basal bird
768 taxa (emu, tinamou, and guinea fowl). *Journal of Experimental Zoology* 311A:586-
769 599.

770 Cleas L, Wolf S, Augat P. 2000. Mechanische Einflüsse auf die Callusheilung. *Chirurg*
771 71:989-994.

772 Colbert EH. 1989. The Triassic dinosaur *Coelophysis*. *Museum of Northern Arizona*
773 *Bulletin* 57:1-160.

774 Cooper RG. 2005. Bacterial, fungal and parasitic infections in the ostrich (Struthio
775 camelus var. domesticus). *Animal Science Journal* 76:97-106.

776 Coria RA, Currie PJ. 2006. A new carcharodontosaurid (Dinosauria, Theropoda) from the
777 Upper Cretaceous of Argentina. *Geodiversitas* 28:71-118.

778 Currie PJ. 2000. Possible evidence of gregarious behavior in tyrannosaurids. *Gaia*
779 15:271-277.

780 Currie PJ, Eberth DA. 2010. On gregarious behavior in *Albertosaurus*. *Canadian Journal of*
781 *Earth Sciences* 47:1277-1289.

782 Currie PJ, Zhao X. 1993. A new carnosaur (Dinosauria, Theropoda) from the Jurassic of
783 Xinjiang, People's Republic of China. *Canadian Journal of Earth Sciences* 30:2037-
784 2081.

785 Currie PJ, Trexler D, Koppelhus EB, Wicks K, Murphy N. 2005. An unusual multi-
786 individual tyrannosaurid bonebed in the Two Medicine Formation (Late
787 Cretaceous, Campanian) of Montana (USA). In: Carpenter K ed. *The carnivorous*
788 *dinosaurs*. Bloomington: Indiana University Press, 313-324.

789 Effron M, Griner L, Benirschke K. 1977. Nature and rate of neoplasia found in captive
790 wild mammals, birds, and reptiles at necropsy. *Journal of the National Cancer*
791 *Institute* 59:185-198.

792 Evers S, Foth C, Rauhut OWM, Pabst B, Mateus O. 2013. Traumatic pathologies in the
793 postcranium of an adult *Allosaurus* specimen from the Morrison Formation of the
794 Howe Quarry, Wyoming, U.S.A. *Journal of Vertebrate Paleontology, Program and*
795 *Abstracts* 33:124.

796 Farke AA. 2004. Horn use in *Triceratops* (Dinosauria: Ceratopsidae): testing behavioral
797 hypotheses using scale models. *Palaeontologia Electronica* 7:1-10.

798 Farke AA, O'Connor PM. 2007. Pathology in *Majungasaurus crenatissimus* (Theropoda:
799 Albelisauridae) from the Late Cretaceous of Madagascar. *Journal of Vertebrate*
800 *Paleontology* 27:180-184.

801 Fiorillo AR. 1998. Bone modification features on sauropod remains (Dinosauria) from
802 the Freezeout Hills Quarry N (Morrison Formation) of southeastern Wyoming and

their contribution to fine-scale paleoenvironmental interpretation. *Modern Geology* 23:111-126.

Foster JR. 2003. Paleoecological analysis of the vertebrate fauna of the Morrison Formation (Upper Jurassic), Rocky Mountain Region, U.S.A. *New Mexico Museum of Natural History and Science, Bulletin* 23:1-95.

Gates TA. 2005. The Late Jurassic Cleveland-Lloyd Dinosaur Quarry as a drought-induced assemblage. *Palaios* 20:363-375.

Gilmore GW. 1920. Osteology of the carnivorous dinosauria in the United States National Museum, with special reference to the genera *Antrodemus* (*Allosaurus*) and Ceratosaurus. *Bulletin of the United States National Museum* 110:1-159.

Gomis SM, Goodhpe R, Kumor L, Caddy N, Riddell C, Potter AA, Allan BJ. 1997. Isolation of *Escherichia coli* from cellulitis and other lesions of the same bird in broilers at slaughter. *The Canadian Veterinary Journal* 38:159-162.

Gross JD, Rich TH, Vickers-Rich P. 1993. Dinosaur bone infection. *National Geographic Research & Exploration* 9:286-293.

Hanna RR. 2002. Multiple injury and infection in a sub adult theropod dinosaur *Allosaurus fragilis* with comparisons to allosaur pathology in the Cleveland-Lloyd Dinosaur Quarry Collection. *Journal of Vertebrate Paleontology* 22:76-90.

Harris JD. 1998. A reanalysis of *Acrocanthosaurus atokensis*, its phylogenetic status, and paleobiological implications, based on a new specimen from Texas. *New Mexico Museum of Natural History and Science, Bulletin* 13:1–75.

824 Hasiotis ST, Fiorillo AR, Hanna RR. 1999. Preliminary report on borings in Jurassic
825 dinosaur bones: evidence for invertebrate-vertebrate interactions. In: Gillette DD
826 ed. *Vertebrate Paleontology in Utah*. Salt Lake City: Miscellaneous Publication, 193-
827 200.

828 Holliday CM, Nesbitt SJ. 2013. Morphology and diversity of the mandibular symphysis of
829 archosauriforms. *Geological Society, London, Special Publications* 379:1-18.

830 Holliday CM, Gardner NM, Paesani SM, Douthitt M, Ratliff JL. 2010. Microanatomy of the
831 mandibular symphysis in lizards: patterns in fiber orientation and Meckel's
832 cartilage and their significance in cranial evolution. *The Anatomical Record*
833 293:1350-1359.

834 Huchzermeyer FW. 2003. *Crocodiles*. Wallingford: CABI Publishing.

835 Huchzermeyer FW, Cooper JA. 2000. Fibricess, not abcess, resulting from a localised
836 inflammatory response to infection in reptiles and birds. *Veterinary Record*
837 147:515-517.

838 Hutchinson JR, Anderson FC, Blemker SS, Delp SL. 2005. Analysis of hindlimb muscle
839 moment arms in *Tyrannosaurus rex* using a three-demensional musculoskeletal
840 computer model: implications for stance, gait, and speed. *Paleobiology* 31:676-701.

841 Klein P, Schell H, Streitparth F, Heller M, Kassi J-P, Kandziora F, Bragulla H, Haas NP,
842 Duda GN. 2003. The initial phase of fracture healing is specifically sensitive to
843 mechanical conditions. *Journal of Orthopaedic Research* 21:662-669.

844 Kobayashi Y, Lü J. 2003. A new ornithomimid dinosaur with gregarious habits from the
845 Late Cretaceous of China. *Acta Palaeontologica Polonica* 48:235–259.

Lambe LM. 1917. The Cretaceous theropodous dinosaur *Gorgosaurus*. *Geological Survey of Canada, Memoir* 100:1-84.

Loboa EG, Beaupré GS, Carter DR. 2001. Mechanobiology of initial pseudoarthrosis formation with oblique fracture. *Journal of Orthopaedic Research* 19:1067-1072.

Loewen MA. 2009. Variation in the Late Jurassic theropod dinosaur *Allosaurus*: ontogenetic, functional, and taxonomic implications. University of Utah.

Madsen JHJ. 1976. *Allosaurus fragilis*: a revised osteology. *Utah Geological and Mineralogical Survey Bulletin* 109:3-163.

Mallison H. 2010. The digital *Plateosaurus* II: An assessment of the range of motion of the limbs and vertebral column and of previous reconstructions using a digital skeletal mount. *Acta Palaeontologica Polonica* 55:433-458.

Marsh OC. 1884. Principal characters of American Jurassic dinosaurs. Part 8. The order Theropoda. *American Journal of Science* 27:329-341.

McCrea RT, Buckley LG, Farlow JO, Lockley MG, Currie PJ, Matthews NA, Pemberton SG. 2014. A "terror of tyrannosaurs": the first trackways of tyrannosaurids and evidence of gregariousness and pathology in Tyrannosauridae. *PLoS ONE* 9:e103613.

McKibbin B. 1978. The biology of fracture healing in long bones. *The Journal of Bone and Joint Surgery* 60:150-162.

Molnar RE. 2001. Theropod paleopathology: a literature survey. In: Tanke DH, Carpenter K eds. *Mesozoic Vertebrate Life*. Bloomington: Indiana University Press, 337-363.

867 Molnar RE, Farlow JO. 1990. Carnosaur paleobiology. In: Weishampel DB, Dodson P,
868 Osmólska H eds. *The Dinosauria*. Berkeley: University of California Press, 210-224.

869 Montali RJ. 1988. Comparative pathology of inflammation in the higher vertebrates
870 (reptiles, birds and mammals). *Journal of Comparative Pathology* 99:1-26.

871 Moodie RL. 1923. *Paleopathology: an introduction to the study of ancient evidences of*
872 *disease*. Urbana: University of Illinois Press.

873 Murphey MD, Choi JJ, Kransdorf MJ, Flemming DJ, Gannon FH. 2000. Imaging of
874 osteochondroma: variants and complications with radiologic-pathologic
875 correlation. *Radiographics* 20:1407-1434.

876 Norell MA, Makovicky PJ. 1999. Important features of the dromaeosaurid skeleton II:
877 information from newly collected specimens of *Velociraptor mongoliensis*. *American*
878 *Museum Novitates* 3282:1-45.

879 Organ CL. 2006. Thoracic epaxial muscles in living archosaurs and ornithopod
880 dinosaurs. *The Anatomical Record, Part A* 288A:782-793.

881 Ortner DJ, Putschar WGJ. 1981. *Identification of pathological conditions in human skeletal*
882 *remains*. Washington, D. C.: Smithsonian Institution Press.

883 Ostrom JH. 1969. Osteology of *Deinonychus antirrhopus*, an unusual theropod from the
884 Lower Cretaceous of Montana. *Peabody Museum of Natural History, Bulletin* 30:1-
885 165.

886 Park S-H, O'Connor K, McKellop H, Sarmiento A. 1998. The Influence of active shear or
887 compressive motion on fracture-healing. *The Journal of Bone and Joint Surgery*
888 80:868-878.

889 Petersen K, Isakson JI, Madsen JHJ. 1972. Perliminary study of paleopathologies in the
890 Cleveland-Lloyd dinosaur collection. *Utah Academy Proceedings* 49:44-47.

891 Peterson JE, Henderson MD, Scherer EP, Vittore CP. 2009. Face biting on a juvenile
892 tyrannosaurid and behavioral implications. *Palaios* 24:780-784.

893 Pschyrembel W. 1990. *Klinisches Wörterbuch*. Berlin: Walter de Gruyter & Co.

894 Raath MA. 1990. Morphological variation in small theropods and its meaning in
895 systemtics: evidence from *Syntarsus rhodesiensis*. In: Carpenter K, Currie PJ eds.
896 *Dinosaur systematics: approaches and perspectives*. Cambridge: Cambridge
897 University Press, 91-105.

898 Ratcliffe HL. 1933. Incidence and nature of tumors in captive wild mammals and birds.
899 *The American Journal of Cancer* 17:116-135.

900 Rega E. 2012. Disease in dinosaurs. In: Brett-Surman MK, Holtz TRJ, Farlow JO eds. *The*
901 *complete dinosaur*. Bloomington: Indiana University Press, 666-711.

902 Remes K. 2008. Evolution of the pectoral girdle and forelimb in Sauropodomorpha
903 (Dinosauria, Saurischia): osteology, myology and function. Ludwig-Maximilians-
904 Universität, München.

905 Rothschild BM. 1987. Diffuse idiopathic skeletal hyperostosis as reflected in the
906 paleontologic record: dinosaurs and early mammals. *Seminars in Arthritis and*
907 *Rheumatism* 17:119-125.

908 Rothschild BM. 1988. Stress fracture in a ceratopsian phalanx. *Journal of Paleontology*
909 62:302-303.

910 Rothschild BM. 1997. Dinosaurian paleopathology. In: Farlow JO, Brett-Surman MK eds.
911 *The complete dinosaur*. Bloomington: Indiana University Press, 426-448.

912 Rothschild BM, Berman DS. 1991. Fusion of caudal vertebrae in Late Jurassic sauropods.
913 *Journal of Vertebrate Paleontology* 11:29-36.

914 Rothschild BM, Martin LD. 1993. *Paleopathology: disease in the fossil record*. Ann Arbor:
915 CRC Press.

916 Rothschild BM, Martin LD. 2006. Skeletal impact of disease. *New Mexico Museum of*
917 *Natural History and Science, Bulletin* 33:1-226.

918 Rothschild BM, Molnar RE. 2008. Tyrannosaurid pathologies as clues to nature and
919 nurture in the Cretaceous. In: Larson P, Carpenter K eds. *Tyrannosaurus rex, the*
920 *tyrant king*. Bloomington: Indiana University Press, 286-304.

921 Rothschild BM, Storrs GW. 2003. Decompression syndrome in plesiosaurs
922 (Sauropterygia: Reptilia). *Journal of Vertebrate Paleontology* 23:324-328.

923 Rothschild BM, Tanke DH. 2005. Theropod paleopathology. In: Carpenter K ed. *The*
924 *carnivorous dinosaurs*. Bloomington: Indiana University Press, 351-365.

925 Rothschild BM, Tanke DH, Ford TL. 2001. Theropod stress fractures and tendon
926 avulsions as a clue to activity. In: Tanke DH, Carpenter K eds. *Mesozoic Vertebrate*
927 *Life*. Bloomington: Indiana University Press, 331-336.

928 Rothschild BM, Tanke DH, Helbling M, Martin LD. 2003. Epidemiologic study of tumors
929 in dinosaurs. *Naturwissenschaften* 90:495-500.

930 Rothschild BM, Tanke DH, Hershkovitz I, Schultz M. 1998. Mesozoic neoplasia: origins of
931 haemangioma in the Jurassic age. *The Lancet* 351:1862.

932 Rothschild BM, Witzke BJ, Hershkovitz I. 1999. Metastatic cancer in the Jurassic. *The*
933 *Lancet* 354:398.

934 Schell H, Epari DR, Kassi JP, Bragulla H, Bail HJ, Duda GN. 2005. The course of bone
935 healing is influenced by the initial shear fixation stability. *Journal of Orthopaedic*
936 *Research* 23:1022-1028.

937 Sekharappa V, Amritanand R, Krishnan V, David KS. 2014. Symptomatic solitary
938 osteochondroma of the subaxial cervical spine in a 52-year-old patient. *Asian Spine*
939 *Journal* 8:84-88.

940 Sereno PC, Beck AL, Dutheil DB, Gado B, Larsson HCE, Lyon GH, Marcot JD, Rauhut OWM,
941 Sadleir RW, Sidor CA et al. 1998. A long-snouted predatory dinosaur from Africa
942 and the evolution of Spinosaurids. *Science* 282:1298-1302.

943 Snively E, Russel AP. 2007a. Functional variation of neck muscles and their relation to
944 feeding style in Tyrannosauridae and other large theropod dinosaurs. *The*
945 *Anatomical Record* 290:934-957.

946 Snively E, Russell AP. 2007b. Craniocervical feeding dynamics of *Tyrannosaurus rex*.
947 *Paleobiology* 33:610-638.

948 Snively E, Cotton JR, Ridgely RC, Witmer LM. 2013. Multibody dynamics model of head
949 and neck function in *Allosaurus* (Dinosauria, Theropoda). *Palaeontologia*
950 *Electronica* 16:1-29.

951 Stromer E. 1915. Ergebnisse der Forschungsreisen Prof. Stromers in den Wüsten
952 Ägyptens. II Wirbeltier-Reste der Baharîje-Stufe (unterstes Cenoman). 3. Das
953 Original des Theropoden *Spinosaurus aegyptiacus* nov. gen., nov. spec.
954 *Abhandlungen der Königlich Bayerischen Akademie der Wissenschaften.*
955 *Mathematisch-physikalische Klasse* 28:1-32.

956 Strube P, Sentuerk U, Riha T, Kaspar K, Mueller M, Kasper G, Matziolis G, Duda GN, Perka
957 C. 2008. Influence of age and mechanical stability on bone defect healing: age
958 reverses mechanical effects. *Bone* 42:758-764.

959 Tanke DH, Currie PJ. 2000. Head-biting behavior in theropod dinosaurs:
960 paleopathological evidence. *Gaia* 15:167-184.

961 Tanke DH, Rothschild BM. 2002. DINOSORES: An annotated bibliography of dinosaur
962 paleopathology and related topics, 1838-2001. *New Mexico Museum of Natural*
963 *History and Science, Bulletin* 20:1-96.

964 Tsuihiji T. 2004. The ligament system in the neck of *Rhea americana* and its implication
965 for the bifurcated neural spines of sauropod dinosaurs. *Journal of Vertebrate*
966 *Paleontology* 24:165-172.

967 Varricchio DJ, Sereno PC, Zhao X, Tan L, Wilson JA, Lyon GH. 2008. Mud-trapped herd
968 captures evidence of distinctive dinosaur sociality. *Acta Palaeontologica Polonica*
969 53:478-567.

970 Vittore CP, Henderson MD. 2013. Brodie abscess involving a tyrannosaur phalanx:
971 imaging and implications. In: Parrish JM, Molnar RE, Currie PJ, Koppelhus EB eds.
972 *Tyrannosaurid paleobiology*. Bloomington: Indiana University Press, 223-236.

973 Witzmann F, Asbach P, Remes K, Hampe O, Hilger A, Paulke A. 2008. Vertebral pathology
974 in an ornithopod dinosaur: a hemivertebra in *Dysalotosaurus lettowvorbecki* from
975 the Jurassic of Tanzania. *The Anatomical Record* 291:1149-1155.

976 Witzmann F, Claeson KM, Hampe O, Wieder F, Hilger A, Manke I, Niederhagen M,
977 Rothschild BM, Asbach P. 2011. Paget disease of bone in a Jurassic dinosaur. *Current*
978 *Biology* 21:R647-R648.

979 Witzmann F, Schwarz-Wings D, Hampe O, Fritsch G, Asbach P. 2014. Evidence of
980 spondyloarthropathy in the spine of a phytosaur (Reptilia: Archosauriformes) from
981 the Late Triassic of Halberstadt, Germany. *PLoS ONE* 9:e85511.

982 Wolff EDS, Salisbury SW, Horner JR, Varricchio DJ. 2009. Common avian infection
983 plagued the tyrant dinosaurs. *PLoS ONE* 4:e7288.

984 Xing L, Bell PR, Rothschild BM, Ran H, Zhang J, Dong Z, Zhang W, Currie PJ. 2013. Tooth
985 loss and alveolar remodeling in *Sinosaurus triassicus* (Dinosauria: Theropoda) from
986 the Lower Jurassic strata of the Lufeng Basin, China. *Chinese Science Bulletin*
987 58:1931-1935.

988 Xing L, Dong H, Peng G, Shu C, Hu X, Jiang H. 2009. A scapular fracture in
989 *Yangchuanosaurus hepingensis* (Dinosauria: Theropoda). *Geological Bulletin of*
990 *China* 28:1390-1395.

991 Zanno LE, Varricchio DJ, O'Connor PM, Titus AL, Knell MJ. 2011. A New troodontid
992 theropod, *Talos sampsoni* gen. et sp. nov., from the Upper Cretaceous Western
993 Interior Basin of North America. *PLoS ONE* 6:e24487.

994
995
996
997
998

999 **Figures**

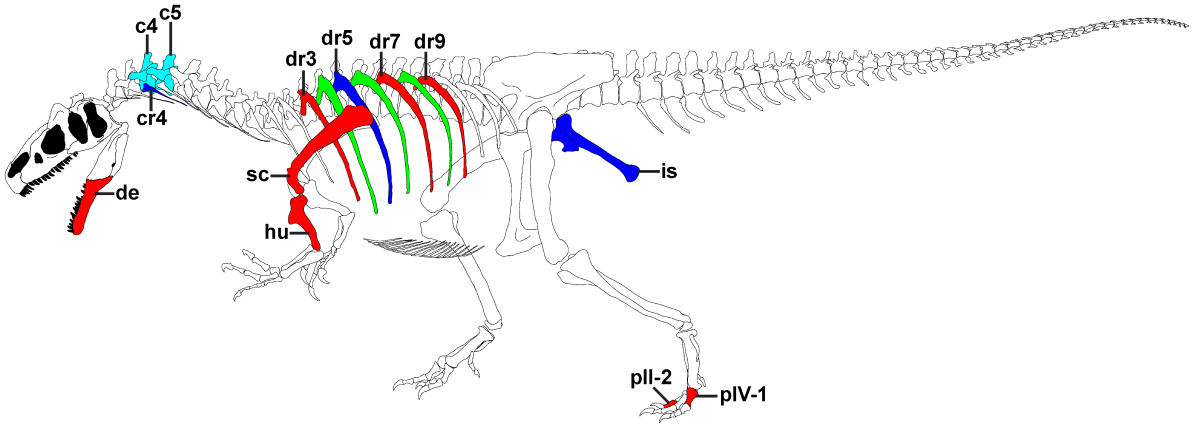

1000

1001 **Figure 1 Overview of pathologies in SMA 0005.** Skeletal reconstruction of SMA 0005,
1002 showing all pathologic bones. Pathologic elements from the left side are shown in red,
1003 while respective elements from the right side are marked in blue. Unpaired pathologic
1004 bones are colored in cyan. Green ribs represent ribs from the left, for which a pathologic
1005 condition is uncertain. **Abbreviations: c** cervical, **cr** cervical rib, **de** dentary, **dr** dorsal
1006 rib, **hu** humerus, **is** ischium, **p** pedal phalanx, **sc** scapula. Skeletal reconstruction of SMA
1007 0005 with courtesy from the Sauriermuseum Aathal.

1008

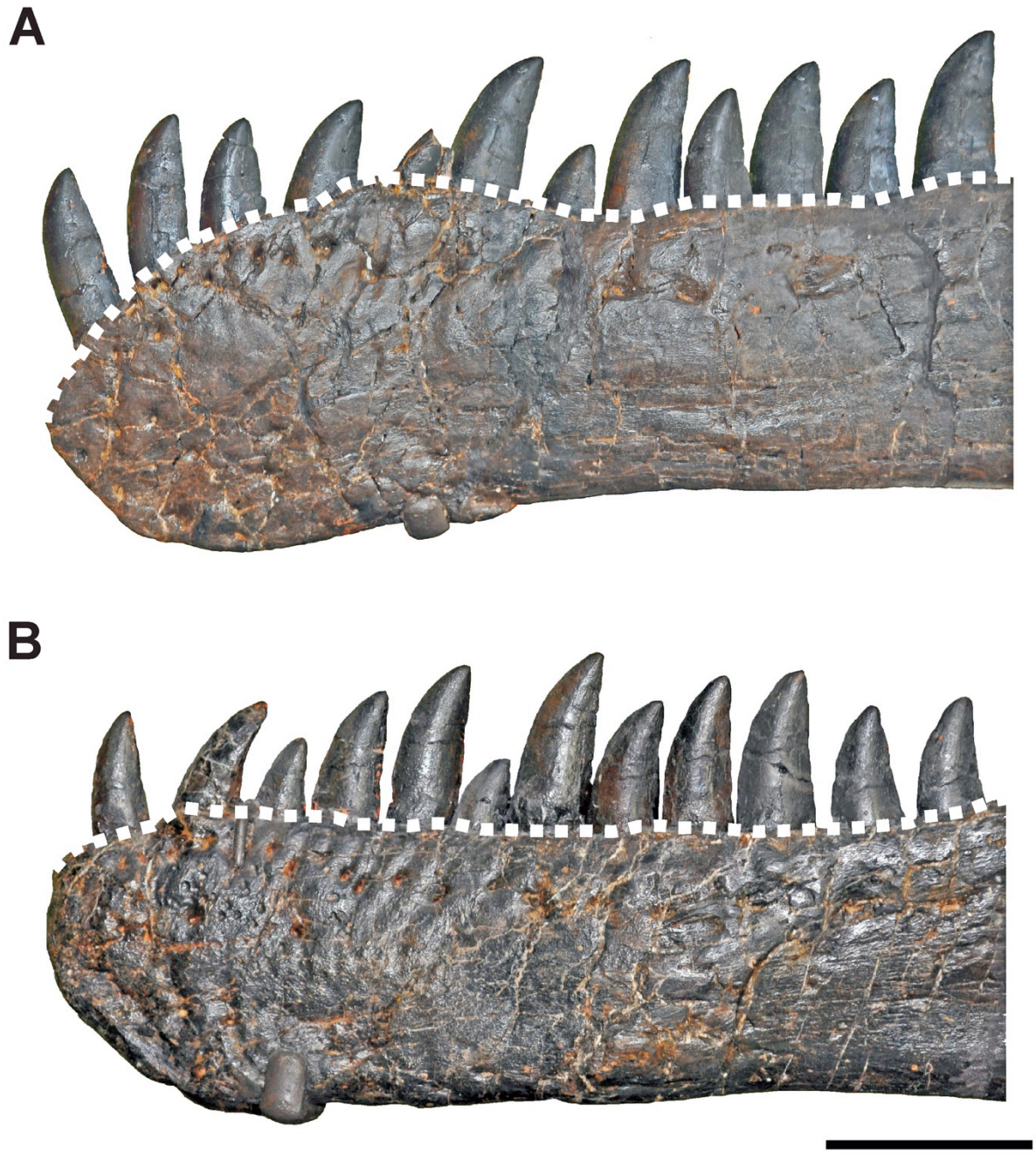

Figure 2 The dentaries of SMA 0005 in lateral view. (A) Left dentary with pathologic anterior end. (B) Right dentary in mirrored view, showing the normal condition for *Allosaurus*. The differences in the shape of the alveolar margin in both dentaries are shown with a dashed line. Note that most teeth in both dentaries are not original, but glued to the internal margin of the dentaries. Scale bar = 5 cm.

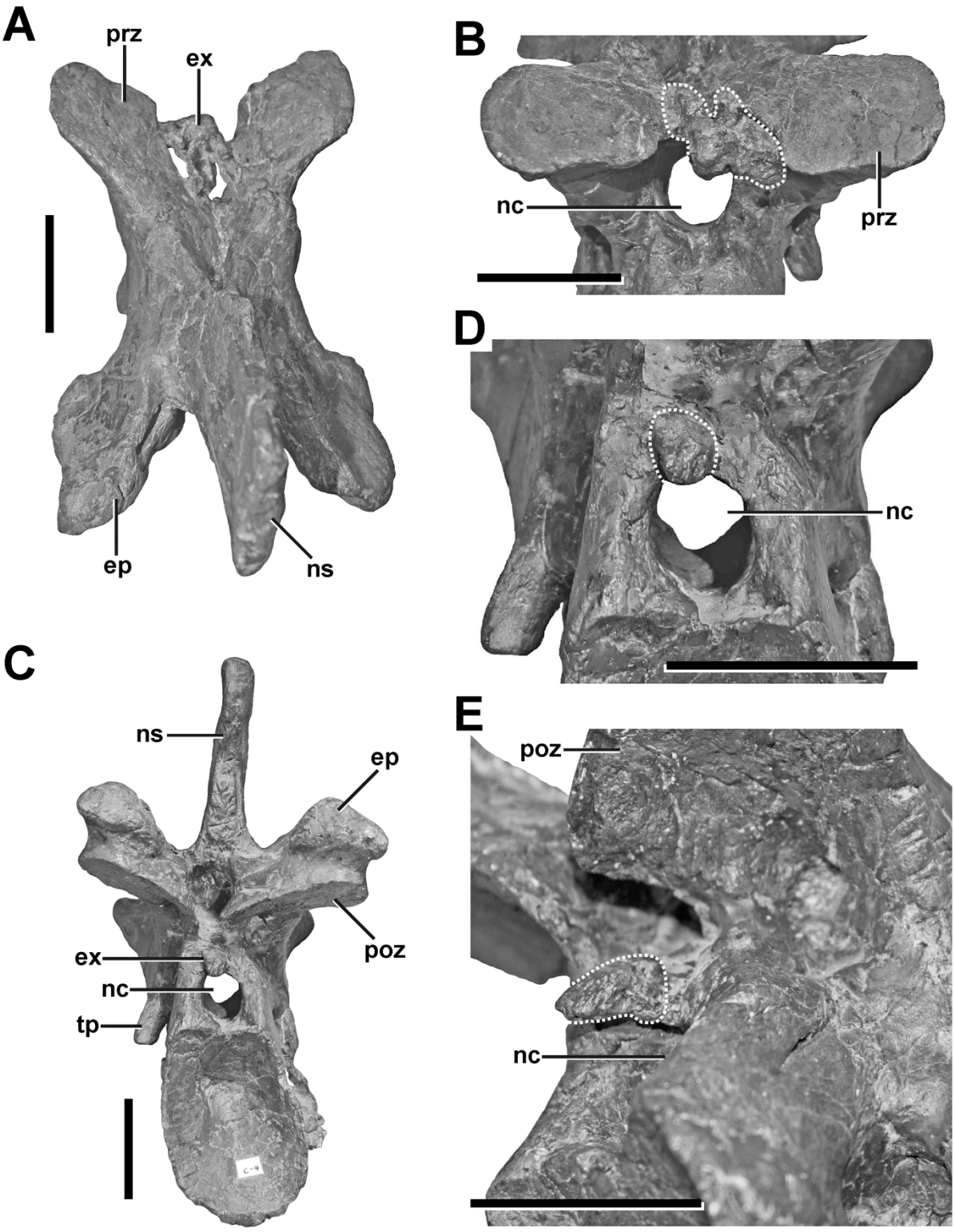

1016

1017 **Figure 3 Fourth cervical of SMA 0005.** (A) Fourth cervical in dorsal view, showing a

1018 pathologic exostosis (possible osteochondroma) between the prezygapophyses. (B)

1019 Possible osteochondroma from anterior view marked by a dotted line. (C) Fourth

1020 cervical in posterior view, showing another exostosis (possible inflammatory

ossification) above the neural canel. (D) Possible inflammatory ossification (dotted line) in close-view. (E) Possible inflammatory ossification (dotted line) in posterolateral view. **Abbreviations: ep** epipophysis, **ex** exostosis, **nc** neural canal, **ns** neural spine, **poz** postzygapophysis, **prz** prezygapophysis, **tp** transverse process. Scale bar = 5 cm.

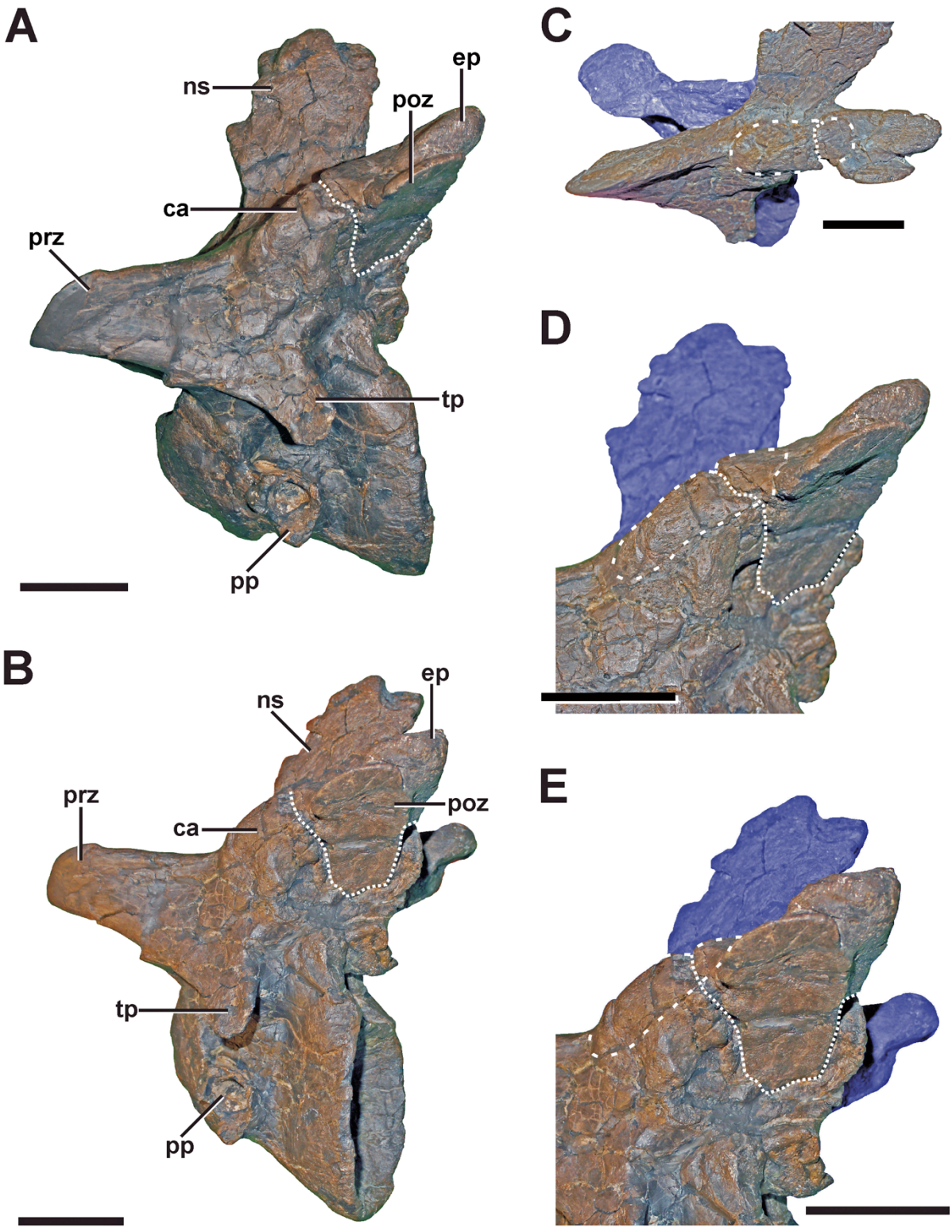

1026

1027 **Figure 4 Fifth cervical of SMA 0005.** (A) Fifth cervical in left lateral view, showing the

1028 callus and the fracture (dotted line) at the base of the left postzygapophysis. (B) Fifth

1029 cervical in lateral view in posterolateral view. (C) Callus (dashed line) and fracture

1030 (dotted line) in laterodorsal view. (D) Callus (dashed line) and fracture (dotted line) in

1031 lateroventral view. (E) Callus (dashed line) and fracture (dotted line) in oblique
1032 posterolateral view. Parts of the bone are colored for better contrast. **Abbreviations: ca**
1033 callus, **ep** epipophysis, **ns** neural spine, **poz** postzygapophysis, **pp** parapophysis, **prz**
1034 prezygapophysis, **tp** transverse process. Scale bar = 5 cm.
1035
1036

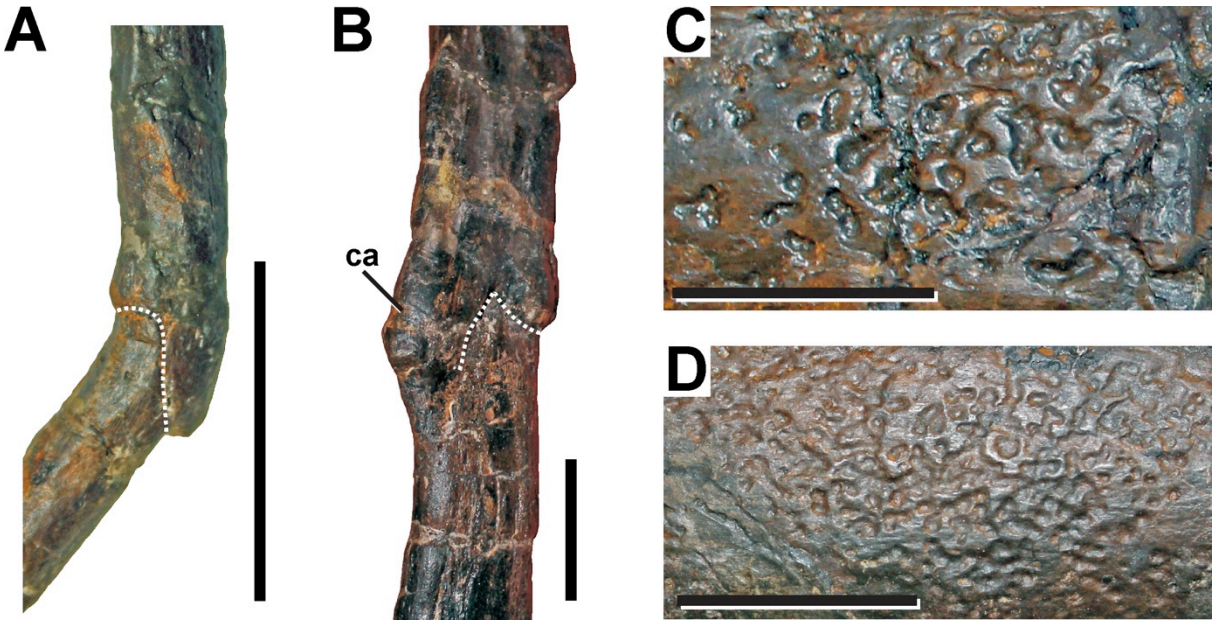

Figure 5 Pathologic ribs and cortical traces in SMA 0005. (A) Fourth cervical rib from the right side with fracture (dotted line). (B) Seventh dorsal rib from the left side with fracture (dotted line). (C) Cortical traces in the right ischium. (D) Cortical traces in the left scapula. **Abbreviations: ca** callus. Scale bar = 2 cm.

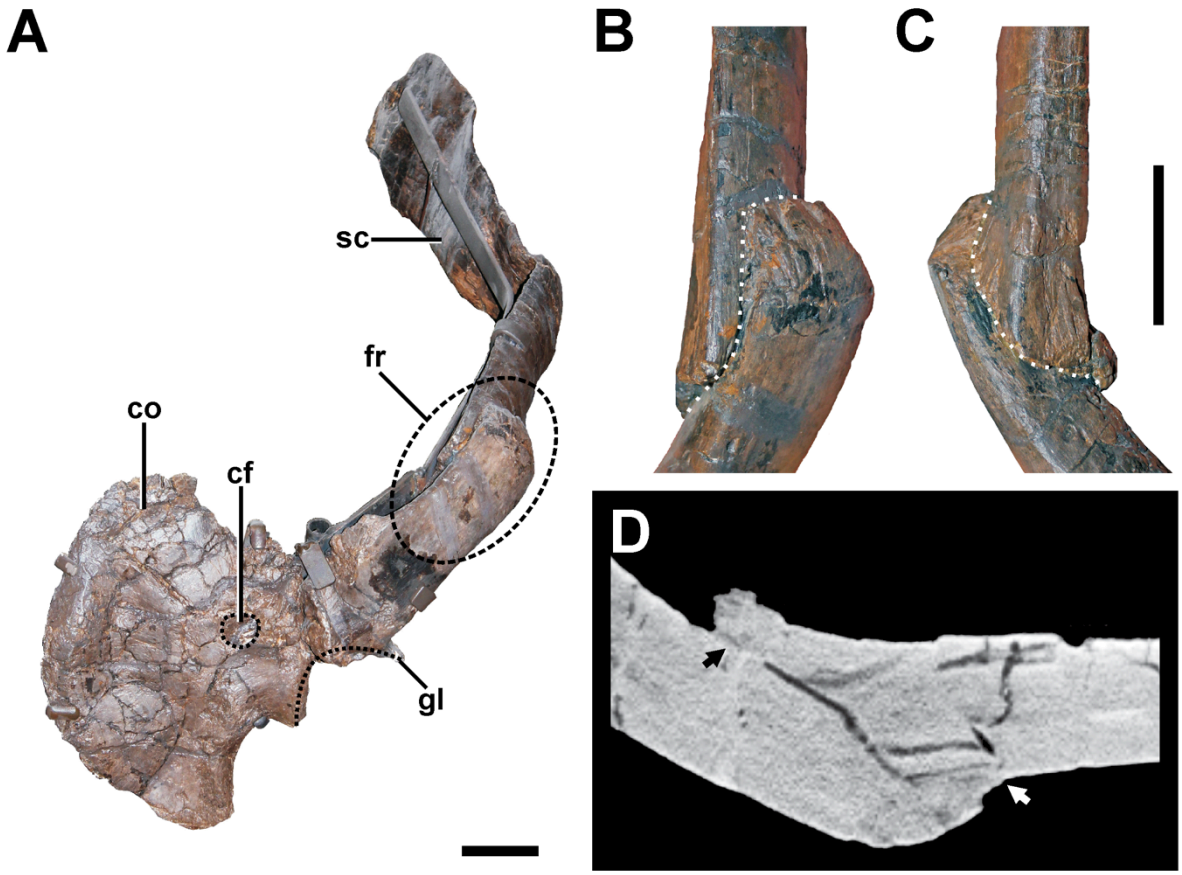

Figure 6 Pathologic scapula of SMA 0005. (A) Left scapula in anterolateral view, showing the fractured area of the scapula blade (dashed line). (B) Fracture (dotted line) in dorsal view. (C) Fracture (dotted line) in ventral view. (D) CT scan of the scapula, showing that only the fracture ends constitute a fused bridge between the fracture elements (arrows), which is consistent with a pseudarthrosis. **Abbreviations: co** coracoid, **cf** coracoid foramen, **fr** fracture, **gl** glenoid facet, **sc** scapula blade. Scale bar = 5 cm.

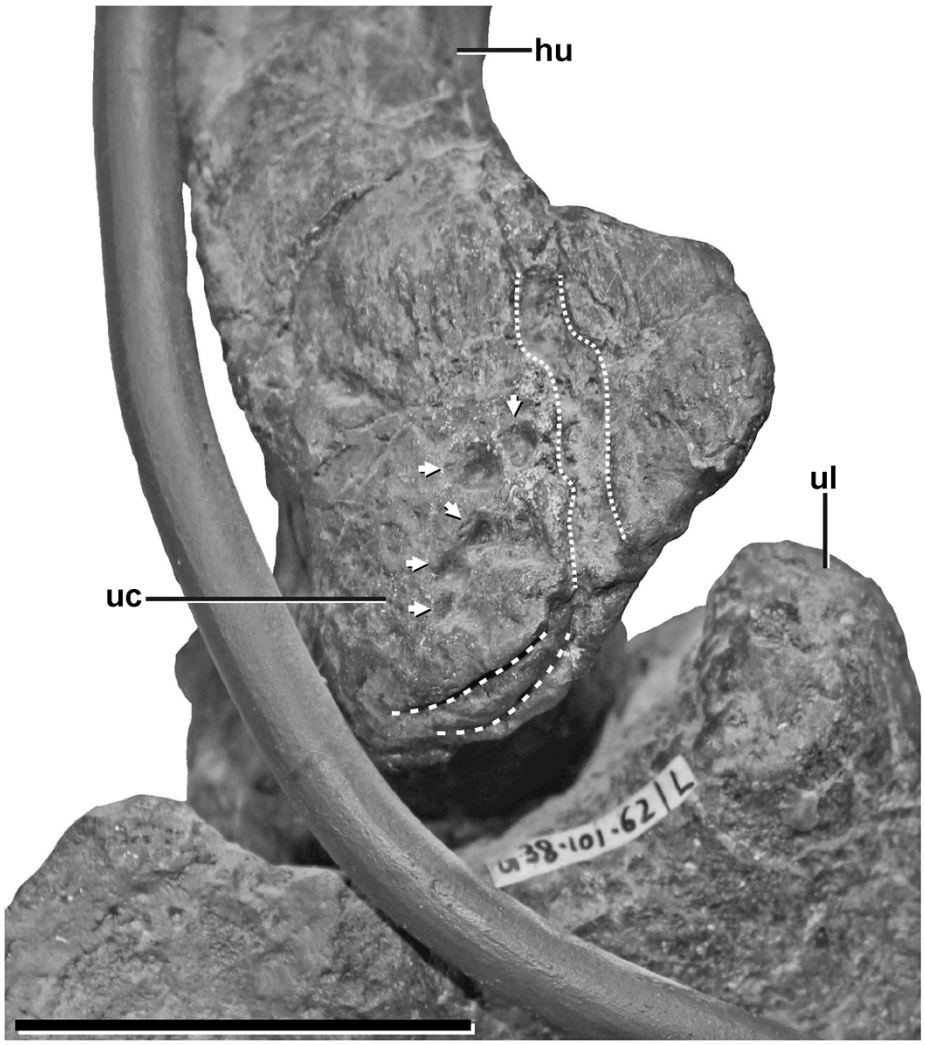

Figure 7 Pathologic structures in the left humerus of SMA 0005. Proximal portion of the humerus in ventromedial view, showing idiopathic pathologies. The pathologies contain an irregular cortical texture with numerous pits (arrows), a deep oblique groove toward the anterior aspect of the medial side (dotted lines), and two sharp, trough-like marks on the ventral surface of the ulnar condyle (dashed lines). **Abbreviations: hu** humerus, **ul** ulna, **uc** ulnar condyle. Scale bar = 5 cm.

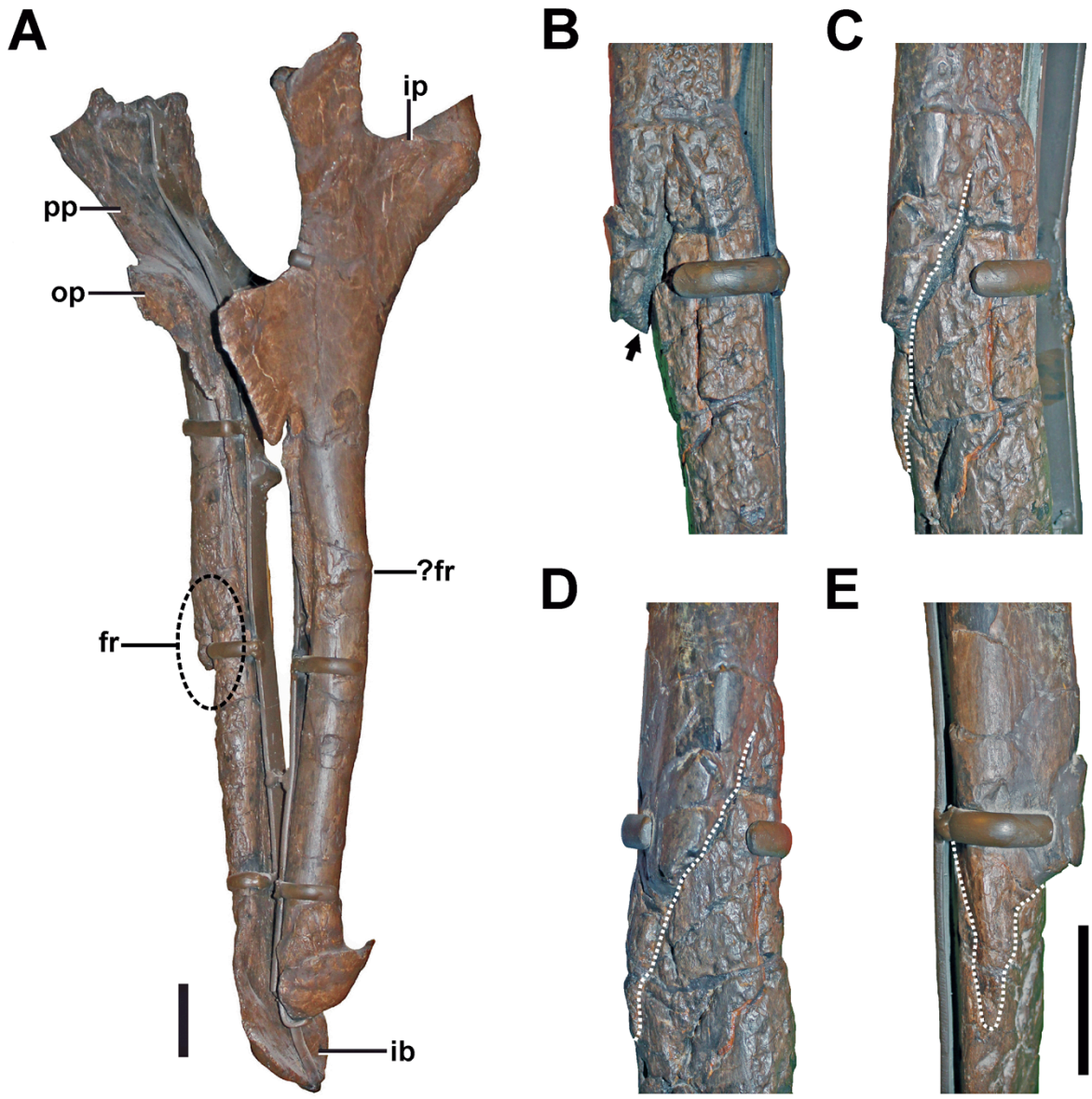

1060

1061 **Figure 8 Ischium of SMA 0005.** (A) Both Ischia in anterolateral view, showing the

1062 oblique fracture at the shaft of the right ischium. (B) Interfragmentary gap (arrow) of

1063 the right ischium in anterior view. (C) Fracture (dotted line) of the right ischium in

1064 anterolateral view. (D) Fracture (dotted line) of the right ischium in lateral view. (E)

1065 Fracture (dotted line) of the right ischium in posterior view. **Abbreviations: fr** fracture,

1066 **ib** ischial boot, **ip** ischial peduncle, **op** obturator process **pp** pubic peduncle. Scale bar =

1067 5 cm.

1068

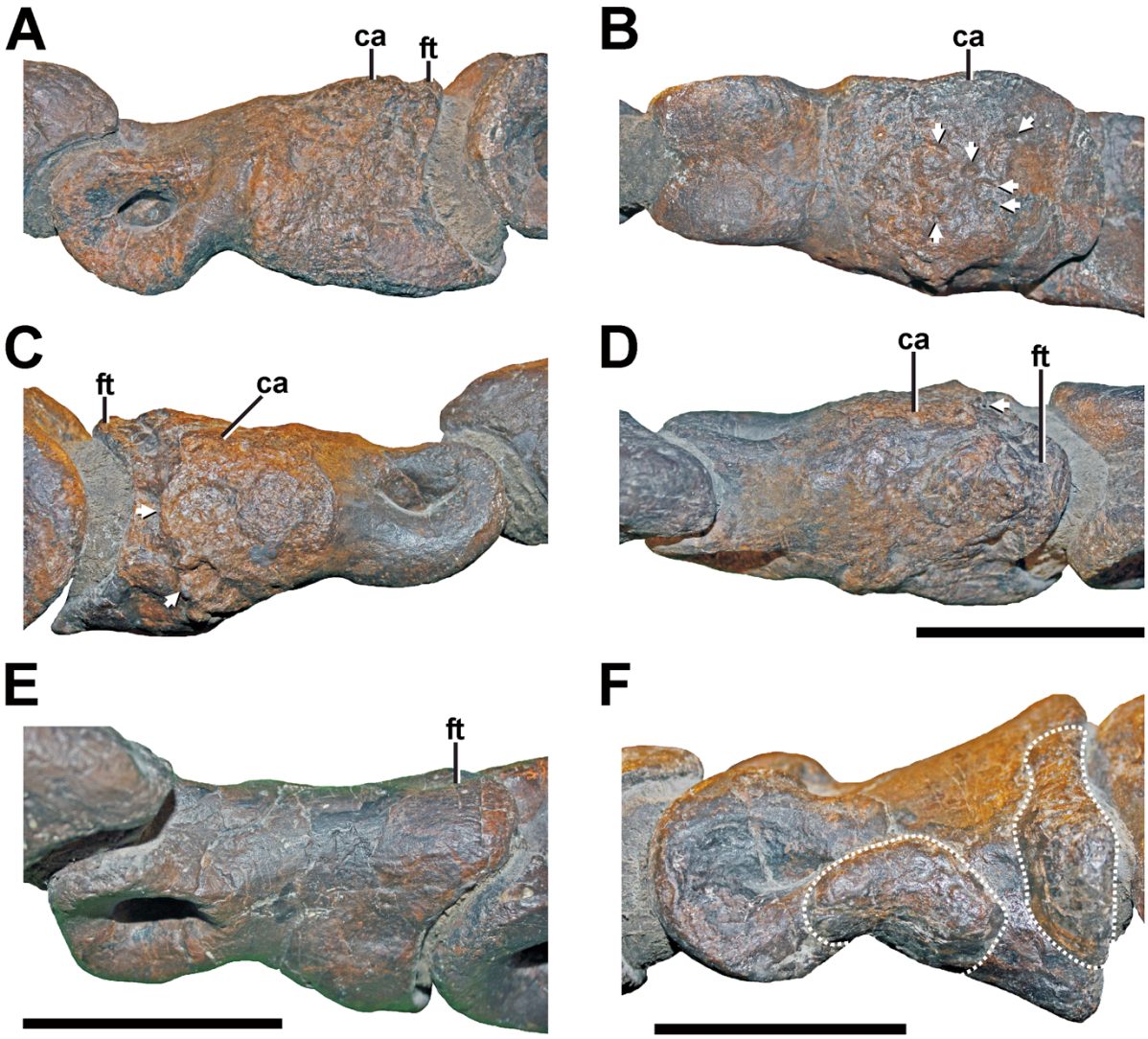

Figure 9 Pathologic phalanges in SMA 0005. (A) Left pedal phalanx II-2 from lateral view, showing the callus and the reduced flexor tubercle. (B) Left pedal phalanx II-2 from ventral view, showing the callus and multiple small pits (arrows). (C) Left pedal phalanx II-2 from medial view, showing the callus and two large depressions (arrows), possibly indicating a secondary infection of the bone. (D) Left pedal phalanx II-2 from dorsal view, showing the callus and one of the two large depressions on the medial side. (E) Right pedal phalanx II-2 from mediodorsal view, showing the normal condition and size of the flexor tubercle. (F) Left pedal phalanx IV-1 in lateral view, showing two idiopathic bulbous swellings (dotted lines). **Abbreviations: ca** callus, **ft** flexor tubercle. Scale bar = 5 cm.

1080

1081